New material of the trechnotherian mammal *Lactodens* from the Early Cretaceous Jehol Biota: Comparison with *Origolestes* and implications for mammal evolution

FANGYUAN MAO, CUNYU LIU, and JIN MENG

A new specimen of *Lactodens sheni*, the only known spalacolestine from the Early Cretaceous Jehol Biota, is reported from the Jiufotang Formation, Liaoning, China. The description focuses on the dental and mandibular morphologies from both the new specimen and the holotype, particularly those that were unknown or poorly known from the holotype when the taxon was established. As revealed primarily by high-resolution computed tomography, morphologies and size gradient of the lower molars and detailed features of the mandibles, such as the masseteric foramen, can be unequivocally described. The dental and mandibular morphologies of *Lactodens* are compared with those of *Origolestes lii*, also from the Jehol Biota; these two taxa represent by far the best specimens in Spalacotheriidae and Zhangheotheriidae, respectively, and could be used as the representatives of their own groups in future higher-level phylogenetic analysis of mammals. The two taxa display considerable differences in dental and mandibular features, probably indicating a deeper split of spalacotheriids and zhangheotheriids than previously thought. Absence of the Meckelian groove in *Lactodens*, contrasting to the distinct one that holds a sizable Meckel's cartilage in adult *Origolestes*, suggests an independent evolution of the definitive mammalian middle ear within "symmetrodontans". The morphological gradient in the tooth row and association of the upper and lower dentitions from the same individual animal are also instructive for interpreting molar variations and evolution in "symmetrodontans" and mammals.

Key words: Mammalia, Symmetrodonta, Spalacotheriidae, Zhangheotheriidae, dental morphology, mandible, middle ear, Cretaceous, Yixian Formation, China.

Fangyuan Mao [maofangyuan@ivpp.ac.cn], Key Laboratory of Evolutionary Systematics of Vertebrates, Institute of Vertebrate Paleontology and Paleoanthropology, Chinese Academy of Sciences, Beijing 100044, China; Division of Paleontology, American Museum of Natural History, New York, New York 10024, USA.
Cunyu Liu [sanyanshishe@163.com], Beipiao Pterosaur Museum of China, Beipiao County, Liaoning Province, 122100, China.
Jin Meng [jmeng@amnh.org] (corresponding author), Division of Paleontology, American Museum of Natural History, New York, New York 10024, USA; Earth and Environmental Sciences, Graduate Center, City University of New York, New York, 10016, USA.

Introduction

"Symmetrodonta" is a group of small Mesozoic mammals, characterized by a simple reversed-triangle molar pattern and has been considered as non-monophyletic (Kielan-Jaworowska et al. 2004). "Symmetrodontans" have been divided into two subgroups: one with "obtuse-angled" molars and the other with "acute-angled" molars. The obtuse-angled "symmetrodontans" are those commonly placed in Kuehneotheriidae and Tinodontidae, some of which are among the earliest members of mammals, such as *Kuehneotherium* (Kermack et al. 1968) and *Woutersia* (Sigogneau-Russell 1983). The acute-angled "symmetrodontans" include two Cretaceous families: Zhangheotheriidae and Spalacotheriidae; they are characterized by possessing molars with relatively acute triangulation that decreases distally in the tooth row (Fox 1976, 1985; Sigogneau-Russell and Ensom 1998; Cifelli 1999; Cifelli and Gordon 1999; Cifelli and Madsen 1999; Cifelli et al. 2014; Ensom and Sigogneau-Russell 2000; Averianov 2002; Gill 2004; Rougier et al. 2003a; Tsubamoto et al. 2004; Hu et al. 1997, 2005a; Lopatin et al. 2005, 2010; Li and Luo

2006; Sweetman 2008; Cuenca-Bescós et al. 2014; Han and Meng 2016). Because of their small size and delicate skeletons, most "symmetrodontans" are known from isolated teeth and/or fragmentary lower jaws; thus, "symmetrodontans" are commonly ignored in general treatments of mammalian relationships, despite their widely acknowledged importance (Cifelli and Gordon 1999). The taxonomic relationships within Zhangheotheriidae and Spalacotheriidae also remained unstable. In general, zhangheotheriids are considered to be more primitive than spalacotheriids (Cifelli and Madsen 1986, 1999; Tsubamoto et al. 2004; Li and Luo 2006; Sweetman 2008; Averianov and Lopatin 2011; Averianov et al. 2013; Bi et al. 2016; Han and Meng 2016; Mao et al. 2020). Despite of the fragmentary nature of fossils and phylogenetic uncertainties, "symmetrodontans" have been considered as an important group because their reversed-triangle molar pattern has been regarded as being intermediate between the "triconodont" tooth pattern in basal mammaliaforms and the tribosphenic pattern that characterizes therians ancestral to marsupials and placentals (Patterson 1956; Hopson and Crompton 1969; Crompton and Sita-Lumsden 1970; Crompton 1971; Cassiliano and Clemens 1979; Hopson 1994; Cifelli and Madsen 1999; Cifelli and Gordon 1999; Rougier et al. 2003a, b). Functionally, the "symmetrodontan" tooth pattern represents a fundamental step in the evolution of mammalian molar design (Kielan-Jaworowska et al. 2004).

Several "symmetrodontans" have been reported from the Jehol Biota. These include *Zhangheotherium quinquecuspidens* (Hu et al. 1997), *Maotherium sinense* Rougier et al. 2003b), *M. asiaticum* (Ji et al. 2009), *Akidolestes cifellii* (Li and Luo 2006), *Anebodon luoi* (Bi et al. 2016), *Lactodens sheni* (Han and Meng 2016) and *Origolestes lii* (Mao et al. 2020). Of these forms, the genera *Akidolestes* and *Lactodens* were placed in Spalacotheriidae and the rest were grouped in Zhangheotheriidae. *Lactodens* is so far the only spalacolestine known from the Jehol Biota.

Spalacolestinae was based on the type genus *Spalacolestes* as a subfamily within Spalacotheriidae (Cifelli and Madsen 1999). This subfamily contains about 10 genera of small insectivores that are recovered from the Cretaceous strata of Europa, Asia, and North America. As in all "symmetrodontans", they are dentally characterized by having the reversed-triangle molar pattern but differ from other "symmetrodontans" in having higher crowned molars with a more acute angle in cusp arrangement in the middle of the tooth series (Cuenca-Bescós et al. 2014). Originally known as a North American endemic group (Patterson 1955; Fox 1976; Cifelli 1990; Cifelli and Madsen 1999), spalacolestines have now been recognized as having a pan-Laurasian distribution during the Cretaceous (Nessov 1997; Averianov 2002; Hu et al. 2005a; Tsubamoto et al. 2004; Sweetman 2008; Cuenca-Bescós et al. 2014; Han and Meng 2016). Most spalacolestine species are represented by fragmentary fossils, commonly isolated teeth. *Lactodens* is the only known spalacolestine that is represented by associated upper and lower teeth, partial cranial and mandibular material, and some postcranial elements from one individual.

Here we report a new specimen of *Lactodens sheni* Han and Meng, 2016, recovered from the Jiufotang Formation at Dapingfang locality, Chaoyang, Liaoning, China, that is close to the type locality Shangheshou. We employed computed tomography to obtain images from the new specimen and the holotype. Our description focuses on the lower molars and other parts that were not preserved or poorly known in the holotype, in the hope that the morphology of *Lactodens* can be better documented. With the new data, we are able to compare the dental and mandibular morphologies between *Lactodens sheni* and *Origolestes lii*, which represent the two main sub-groups of "symmetrodontans," the zhangheotheriids and spalacotheriids, respectively. Because each species is based on relatively complete material from more than one specimen, the characters and variation displayed in the two taxa are better sampled; as such, the two taxa could serve as representatives for "symmetrodontans" in higher-level phylogenetic analyses of mammals. We further discuss implications of the new data to the general evolution of mammals, including the dentition and the middle ear.

Institutional abbreviations.—HG-M, Bohai University Paleontology Center, Jinzhou City, Liaoning Province, China; IVPP, Institute of Vertebrate Paleontology and Paleoanthropology, Chinese Academy of Sciences, Beijing, China; ZGY, Beipiao Pterosaur Museum of China, Beipiao, China.

Other abbreviations.—DMME, definitive mammalian middle ear; OMC, ossified Meckel's cartilage; TMME, transitional mammalian middle ear. We follow standard convention in abbreviating tooth families as I, C, P, and M, with upper and lower case letters referring to upper and lower teeth, respectively.

Material and methods

The new specimen (ZGY0053, Fig. 1) is represented by a partial skeleton preserved in a pair of split slabs. While much of the skeletal remains was broken, the mandibles and teeth were preserved in good condition, supplementing additional morphologies to the holotype (HG-M016, Fig. 2A). As in the holotype, it is highly probable that the upper and lower dentitions were preserved roughly in their anatomical positions so that the corresponding pairs of upper and lower teeth and their occlusal relationships can be observed and interpreted with confidence. Unlike the holotype that has been needle-prepared to provide access to the teeth embedded in the matrix, we avoided preparing the new specimen because of its small size and fragile remains. We employed computed tomography (CT) and laminography (CL) to obtain the internal morphologies of the mandibles as well as the morphology of dental and mandibular parts that are still embedded in
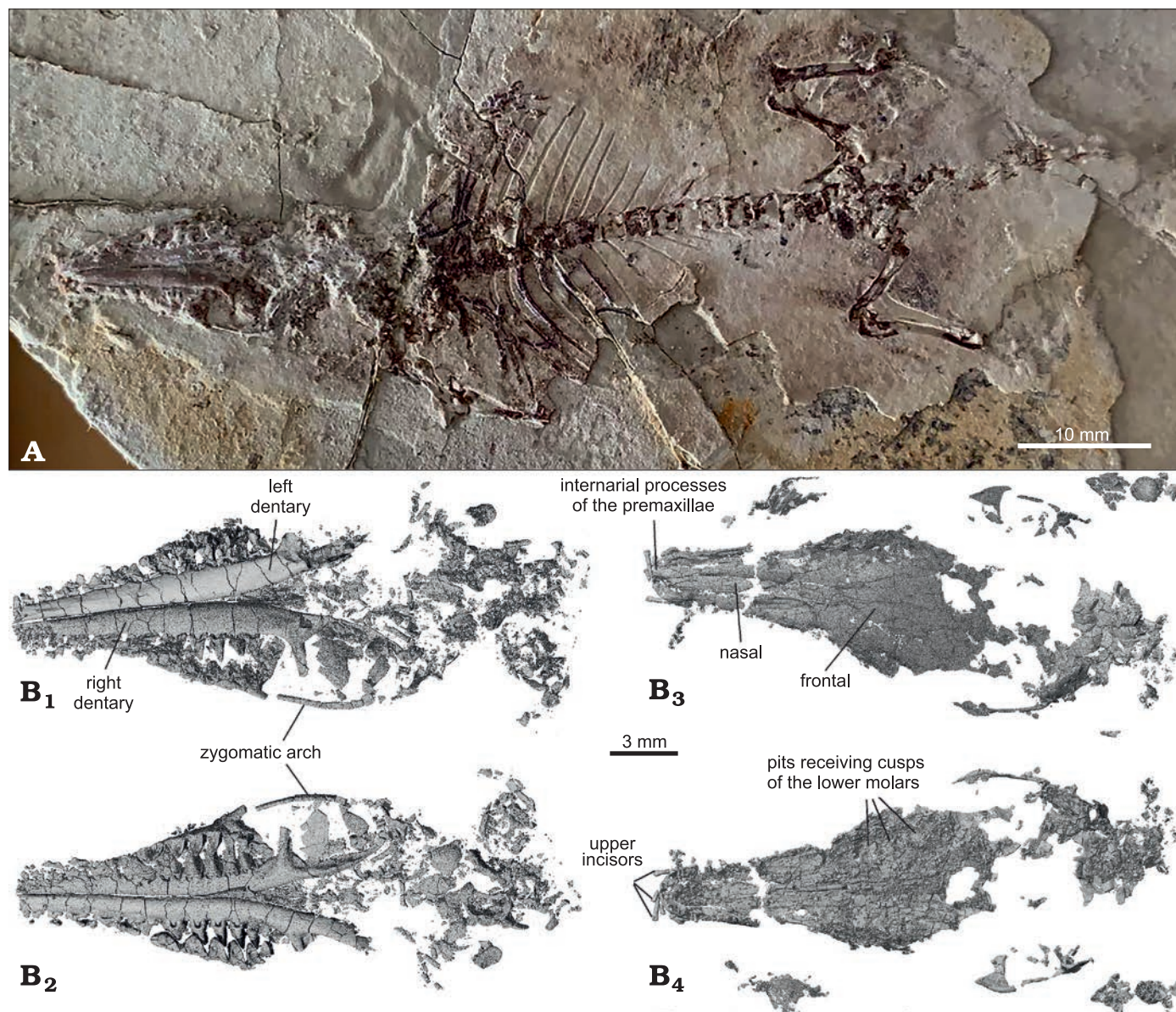
Fig. 1. New specimen of *Lactodens sheni* Han and Meng, 2016 (ZGY0053) from Aptian, Lower Cretaceous Jiufotang Formation of Dapingfang, Caoyang City, Liaoning Province, China. **A**. Partial skeleton in dorsal view that is preserved in the main slab. **B**. CT rendered partial skull; mostly ventral portion with teeth in dorsal (B$_1$) and ventral (B$_2$) views and mainly the skull roof in dorsal (B$_3$) and ventral (B$_4$) views.

the matrix for both the new specimen and the holotype. We also include the zhangheotheriid *Origolestes lii* Mao, Hu, Li, Wang, Chase, Smith, and Meng, 2020, in the comparison, with the focus on IVPP V13604, the specimen for which the best images of tooth morphology were provided; other specimens of *O. lii* were presented in Mao et al. (2020).

Imaging and figures.—Optical images of the new specimen (ZGY0053) were taken using a Canon Digital camera with a macro lens. All the high-resolution micro-CT scanning for the two specimens (HG-M016 and ZGY0053) was conducted using a GE v|tome|x m dual tube 240/180kV system (General Electric, Fairfield, CT, USA) in the Yinghua Inspection and Testing (Shanghai) Co., Ltd and the Key Laboratory of Vertebrate Evolution and Human Origins, Chinese Academy of Sciences. The two specimens were scanned using the

240kv microfocus tube at resolution of a 9.53 μm per voxel for the skeleton of HG-M016 using beam energy for 140 kV and 120 μa, 5.204 μm per voxel for the skull of ZGY0053 using beam energy for 140 kV and 140 μa.

To improve the signal-to-noise ratio, 1800 projections were collected, for 333–2000 ms and averaged 2 times. Sometimes, to accommodate the length of the specimen, 2 total areas were scanned in the Y-axis (multiscan) of ZGY0053 to produce the final projection stack, reconstructed using Phoenix datos|x (General Electric, Wunstorf, Germany). All of the segmentation and the rendering of the CT scanning data were processed using VG Studio Max 3.4 (Volume Graphics, Heidelberg, Germany).

Measurements.—Because the teeth and mandibles are small and partly embedded in the matrix, the measurements
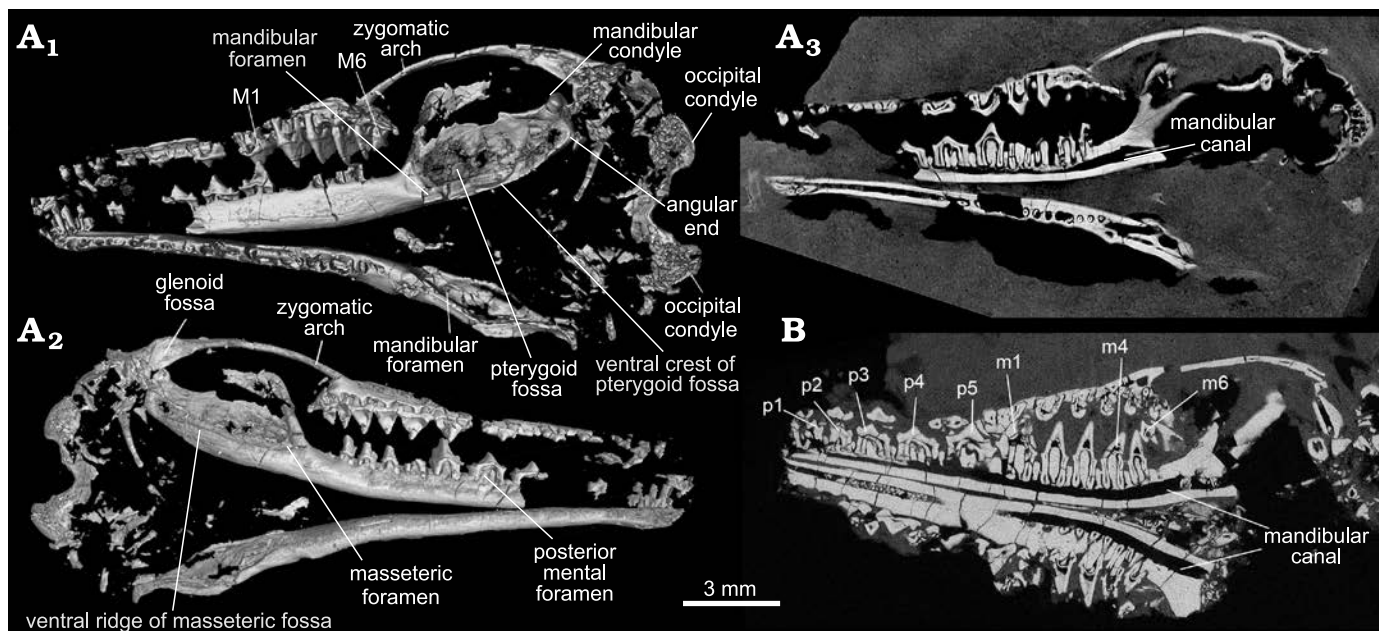
Fig. 2. CT-images of the trechnotherian mammal *Lactodens sheni* Han and Meng, 2016, from Aprian, Lower Cretaceous Jiufotang Formation, Caoyang City, Liaoning Province, China. **A**. Holotype (HG-M016) from Shangheshou area; A₁, virtual skull remains with the lingual side of the right mandible exposed (see Han and Meng 2016: fig. 1); A₂, virtual skull remains with the lateral side of the right mandible exposed (this side of the skull is embeded in the matrix and not visible except for the part of cheek teeth that were needle-prepared from the back side of the slab (Han and Meng 2016: figs. 1, 5); A₃, a CT-slice showing the contrast of bone and matrix and revealing the roots of some teeth. **B**. ZGY0053 from Dapingfang, a CT-section through the skull (showing the root conditions). Note there is no tooth germ under any cheek teeth in both specimens in A₃ and B.

Table 1. Measurements (in mm length/width and angular degree of the trigon and trigonid) of the teeth of *Lactodens sheni* Han and Meng, 2016 (ZGY0053). *, estimated; ?, unknown.

Teeth		Left	Right
Upper	I3	0.248*/0.174*	?
	C	0.209*/0.268*	0.47*/0.231*
	P1	0.564*/0.327	0.853/0.261
	P2	0.955/0.362	0.903/0.314
	P3	1.19/0.41	1.189/0.446
	M1	1.448/0.729 (107°)	1.468/0.756 (125°)
	M2	1.232/0.827 (74°)	1.203/0.946 (67°)
	M3	1.051/1.036 (55°)	1.009/1.081 (49°)
	M4	0.909/1.147 (47°)	0.886/1.137 (40°)
	M5	0.828/1.109 (45°)	0.788/1.083 (41°)
	M6	0.564/0.648 (41°)	0.558/0.739 (41°)
Lower	c	0.351/0.179	0.355/0.157
	p1	0.582/0.216	0.541/0.179
	p2	0.716/0.216	0.698/0.237
	p3	1.087/0.311	1.064/0.326
	p4	1.374/0.395	1.361/0.342
	p5	1.604/0.611	1.56/0.5
	m1	1.258/0.803 (104°)	1.286*/0.65* (?)
	m2	0.888/0.962 (61°)	0.91/0.813 (63°)
	m3	0.838/0.984 (49°*)	0.831/0.906 (50°)
	m4	0.877/1.002 (56°)	0.878/0.75 (62°*)
	m5	0.643*/0.638* (42°*)	0.756/0.72 (56°)
	m6	0.481/0.487 (85°)	0.542/0.358 (72°)

were taken using digital methods from the CT images of the specimen. Linear measurements were taken using the Measurements Menu/Coordinate Measurement module in VGStudio Max 3.4 and/or ImageJ. Each measurement was repeated three times, and the average was used. The measurements are listed in Table 1.

Terminology.—We follow Kielan-Jaworowska et al. (2004) for the use of "symmetrodontans" as a descriptive term, knowing that "symmetrodontans" probably do not form a monophyletic group. We follow Rougier et al. (2003a) for the use of Zhangheotheriidae as a family, which was defined as the group "formed by the common ancestor of *Zhangheotherium* and *Maotherium* and all its descendants", although the monophyly of this taxon has not been consistently established (Li and Luo 2006; Sweetman 2008; Averianov et al. 2013; Han and Meng 2016; Mao et al. 2020); thus, we place Spalacotheriidae directly under Trechnotheria. Dental terminology follows Han and Meng (2016: fig. 2), which is based on several studies (see references therein). We follow Rougier et al. (2003b) for identification of cusp B (the cusp mesial to cusp A) in the upper molar of *Origolestes lii*; the homology of this cusp is still uncertain.

Geological setting

The holotype and the new specimen (ZGY0053) of *Lactodens sheni* are both from the Jiufotang Formation, with the former from a nearby Shangheshou locality in Caoyang City,
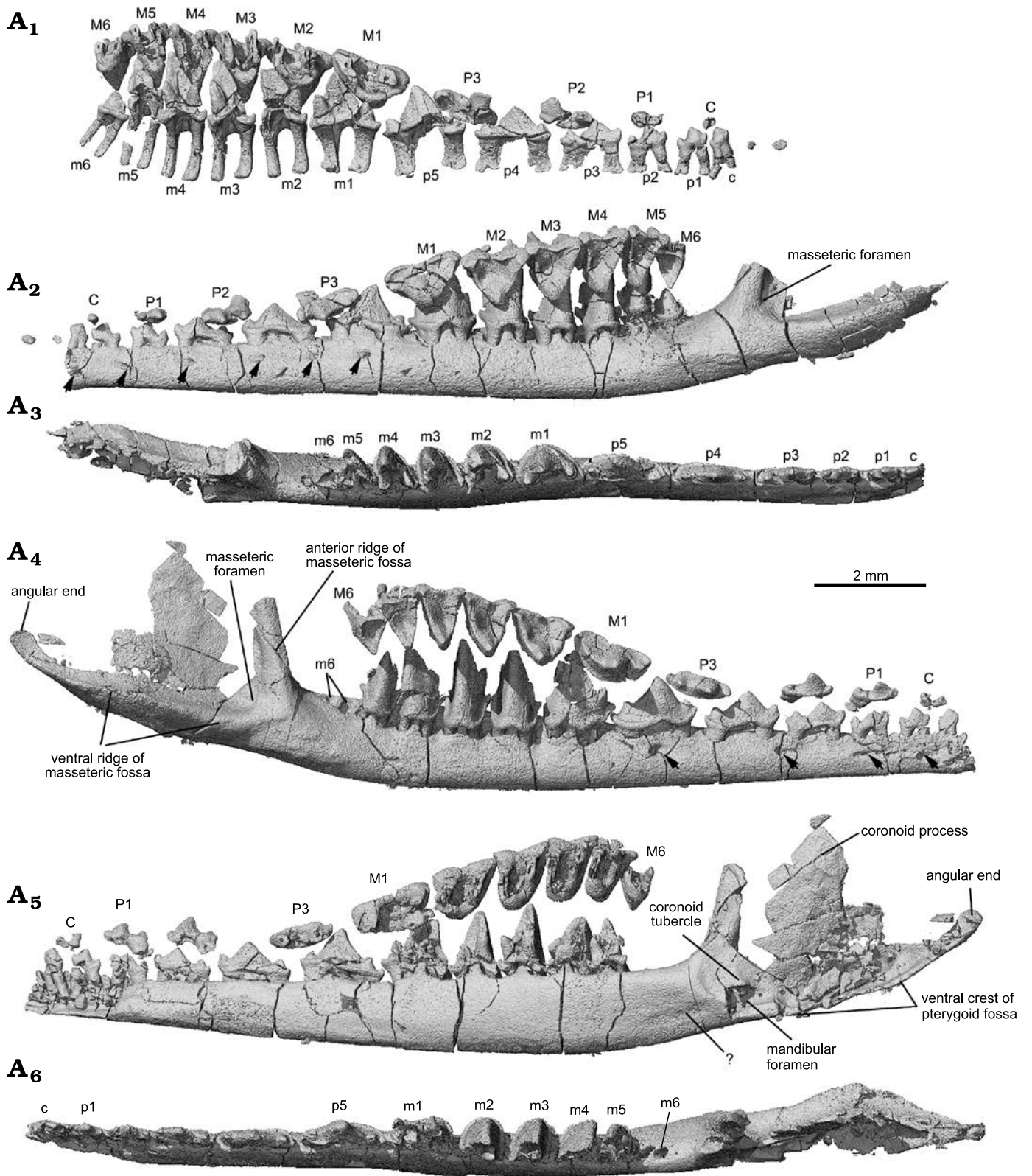
Fig. 3. CT-rendered lower jaws and dentitions of the trechnotherian mammal *Lactodens sheni* Han and Meng, 2016 (ZGY0053), from Aptian, Lower Cretaceous Jiufotang Formation of Dapingfang, Caoyang City, Liaoning Province, China. A_1–A_3, left upper and lower dentition and dentary in medial (only teeth), lateral, and occlusal views, respectively. A_4–A_6, right upper and lower dentition and dentary in lateral, medial, and occlusal views, respectively. Note: angular end is not the mandibular condyle (see Fig. 6); coronoid tubercle, mis-labelled as "cp" in Han and Meng (2016: fig. 10). Upper and lower teeth in A_1, A_2, A_4, A_5 are in the original position that were preserved. Arrows in A_2, A_4 point to mental foramina (note the difference between the two mandibles). Question mark in A_5 points to a faint groove that is not the Meckelian groove (compared to that of *Origolestes lii* in Fig. 6B).

Liaoning Province. The Jehol Biota consists of fossils from Jiufotang, Yixian (west Liaoning), and Huajiying (Hebei) formations; these lithological units range chronologically from the youngest to the oldest (Pan et al. 2013; Yang et al. 2020) and the temporal interval was considered to be at least 10 Ma (130–120 Ma) (Pan et al. 2013) or 15 Ma (135–120 Ma) (Yang et al. 2020) with the lower Jiufotang Formation constrained as ~120 Ma (He et al. 2004; Chang et al. 2009). Fossils from the three lithological units were considered representing three evolutionary stages, with the Jiufotang stage being the youngest (Yang et al. 2020). In addition to *Lactodens sheni*, other mammals from the Jiufotang Formation include the eutriconodontan *Liaoconodon hui* (Meng et al. 2011) and the multituberculates *Jeholbaatar kielanae* (Wang et al. 2019) and *Sinobaatar pani* (Mao et al. 2020). Most recently, the tritylodontid *Fossiomanus sinensis* (Mao et al. 2021) has been reported from the Jiufotang Formation and was considered to be one of the youngest known tritylodontids, probably younger than the tritylodontid from the Kuwajima Formation (Barremian–Aptian) in central Japan (Matsuoka et al. 2016); thus, *F. sinensis* represents the most recent relictual member of non-mammaliaform synapsids known to date.

Systematic palaeontology

Mammalia Linnaeus, 1758

Trechnotheria McKenna, 1975

Spalacotheriidae Marsh, 1887

Spalacolestinae Cifelli and Madsen, 1999

Genus *Lactodens* Han and Meng, 2016

Type species: *Lactodens sheni* Han and Meng, 2016, monotypic; see below.

Diagnosis.—As for the type species.

Lactodens sheni Han and Meng, 2016

Figs. 1–5.

Holotype: HG-M016, a partial skeleton with partial cranium and associated dentaries.

Type locality: Dapingfang, Caoyang City, Liaoning Province, China.

Type horizon: Aptian, Lower Cretaceous Jiufotang Formation.

Material.—Holotype and new specimen (ZGY0053), a partial skeleton with partial cranium and associated mandibles from Early Cretaceous (Aptian) Jiufotang Formation, Shangheshou area, Caoyang City, Liaoning Province, China.

Emended diagnosis.—A spalacolestine with the dental formula I3-C1-P3-M6/i3-c1-p5-m6, double-rooted upper and lower canine and postcanine teeth, distinct diastemata present between upper premolar series but absent in the lower series, extremely low-crowned and transversely narrow premolars, M1 and m1 with wide angulation that decreases distally, ultimate molars considerably smaller than penultimate ones, cusp C weak in mesial upper molars, mandibular condyle without a neck, presence of the masseteric foramen

and lack of the Meckelian groove on the medial rear surface of the dentary bone.

Description.—*Cranium* (Figs. 1, 2): The skull of ZGY0053 was split along the horizontal plane so that the mandible and nearly all teeth were preserved in the main slab and the skull roof, the palate, some dorsal cranial parts, and a few incisors were preserved in the counterpart. Although the cranium was fractured, its general shape in dorsal or ventral view is discernable, similar to that of the holotype. It has a narrow and long rostrum with the facial region gradually flaring toward the zygomatic arch. The arch is slim with its anterior root lateral to M6 and gently curves and ends posteriorly to the glenoid fossa, as shown in the holotype. The glenoid fossa is shallow with its lateral edge more convex than its medial edge and bounded posteriorly by a low postglenoid process or ridge. The occipital condyles are proportionally large, oval-shaped, and widely separated so that the foramen magnum appears large. The anterior edge of the foramen magnum forms a curved notch that intrudes anteriorly in the basioccipital. The rest of the basicranial region in both specimens is too fragmentary to be informative.

On the dorsal side (in the counterpart of the slab), the nasals, frontals and maxillae are preserved; the nasals are narrow and long and expand posteriorly. The anterior portions of the frontals form a triangular wedge that inserts between the nasals. In the rostrum the internarial process, a narrow bar formed by the premaxillae, is present and separates the external nares into two openings. It was previously proposed that the reduction of the internarial process and the concomitant coalescence of the nares into a single apertura nasi are new features of euriconodonts, multituberculates and crown mammals (Ruf et al. 2014; references therein). Thus, if identified correctly, this internarial process represents a primitive condition in mammals. On the ventral side of the rostrum, the alveoli of the incisors show that the upper incisors are separated by small diastemata and I2 is the largest one of the three upper incisors. A few small loose teeth are presumably upper incisors except for a double-rooted one that may be the canine. On the palate, which is heavily fractured, there are signs of pits lingual to the upper molars; these are likely the pits for receiving the tall cusps of the lower molars, a feature observed in some other Mesozoic taxa, such as species of *Origolestes* (Mao et al. 2020), *Morganucodon* (Jäger et al. 2019), and *Repenomamus* (Hu et al. 2005b).

Mandible (Figs. 1–3, 6): In ZGY0053 the two mandibles and most teeth are preserved in the main slab. Because the skull roof was peeled off (preserved in the counterpart slab), the exposed skull fragments and roots of upper teeth are exposed in dorsal view. The two mandibles were flipped down medially in preservation and their lingual sides are exposed in the main slab (Fig. 1). The buccal sides of all mandibles in the holotype and the new specimen are embedded in the matrix so that the morphology in this view was little known when *Lactodens sheni* was first reported (Han and Meng 2016); it became available owing to CT-imaging in this study.
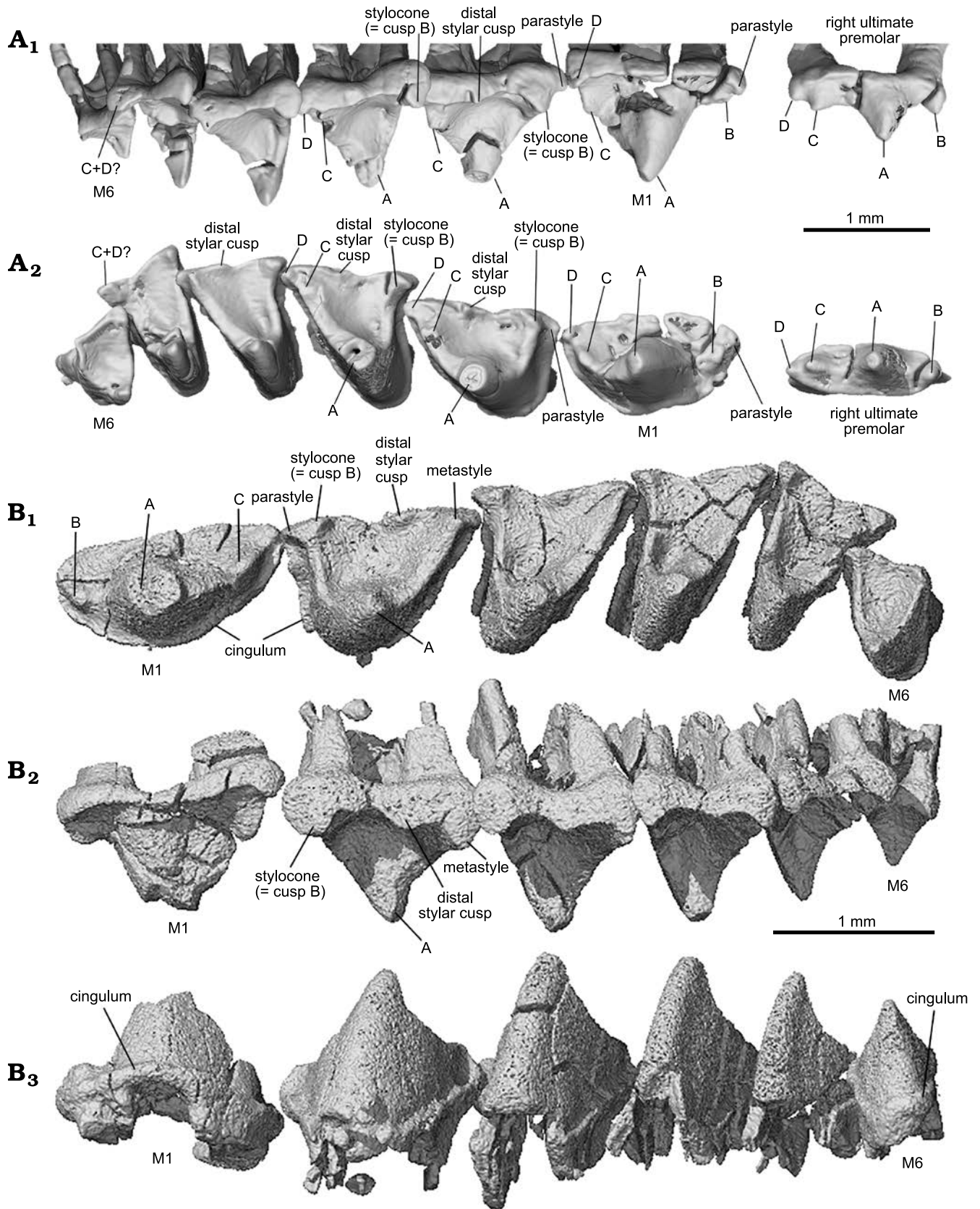
Fig. 4. Upper molars of the trechnotherian mammal *Lactodens sheni* Han and Meng, 2016, from Aptian, Lower Cretaceous Jiufotang Formation, Caoyang City, Liaoning Province, China. **A**. Holotype (HG-M016) from Shangheshou area; right ultimate premolar and M1–M6 in buccal (A₁) and occlusal (A₂) views, showing the corresponding cusps on different teeth. **B**. ZGY0053 from Dapingfang; left upper molars (M1–M6) in occlusal (B₁), buccal (B₂), and lingual (B₃) views. Image in B₃ is horizontally flipped for convenience of comparison.

Compared to a slender and long horizontal ramus the masseteric fossa is broad; it is delimited by a blunt anterior ridge and a ventral ridge that is blunt anteriorly and crest-like posteriorly. The ultimate lower molar is mesial to the anterior ridge. On the medial surface of the dentary, there is no Meckelian groove, as noted in the holotype (Han and Meng 2016). There is a faint groove when the mandible is viewed with the light coming in certain angles (see Fig. 3A$_6$), but this is certainly not the Meckelian groove. At the root of the anterior ridge the masseteric foramen opens in the anterior end of the fossa. The posterior end of the fossa is squared up and the posteroventral corner is bounded by thickened bone that may be misinterpreted as the condyle if only this part was preserved (Fig. 3A$_4$). We term this thickened area as the "angular end" (Figs. 2, 6). The condyle is dorsal to the angular end and does not have a neck; it is transversely widened and has a convex articular surface. The coronoid process is broad and tilts at about 64° (measured as the smaller angle between the anterior ridge of the process and the horizontal axis through the alveoli; or the larger angle is 116°; Han and Meng 2016). The mandibular notch, the space between the coronoid process and the condyle, is broad and shallow. There are multiple mental foramina on the buccal surface of the mandible and the number varies even in the two mandibles of the ZGY0053, in the left mandible there are at least six mental foramina. The posterior-most one, also the largest one, is consistently below p5 in the ZGY0053 mandibles and in the holotype. Each mental foramen leads anteriorly to a narrow groove.

CT-scans revealed that there are two roots for each upper or lower postcanine tooth, arranged mesiodistally. The roots are short relative to the height of the tooth crown and flare at the distal ends. The roots of the lower teeth end the roof of the mandibular canal. There is no evidence for tooth germs of erupting teeth in the dentary bone under the upper and lower dentition. The rest of the mandible of *Lactodens sheni* has been described by Han and Meng (2016).

Upper teeth (Figs. 3, 4, 7): In the ZGY0053 the tip of the skull was broken so that the upper incisors were poorly preserved in the counterpart slab, whereas only fragments of lower incisors were preserved. The canines and postcanine teeth in both the upper and lower jaws are in good condition and show the same tooth formula and similar tooth morphologies as in the holotype, which allow us to assign the new specimen to *Lactodens sheni* (Han and Meng 2016). The new specimen confirms some unusual features observed in the holotype, such as the relatively large diastemata between the upper premolars, different upper and lower premolar numbers, and the low crown premolars that have the shape of deciduous teeth. In addition to the dental morphology and diastema that were used to distinguish the molars from premolars, we add here that the two roots of the molars are more closely positioned mesiodistally, each being transversely widened, compared to those of the premolars. However, the identification of the tooth as M1 instead of P4 is based on our understanding of the tooth morphologies

(Han and Meng 2016; this study); this tooth may prove to be a P4 in future study.

With the CT-scan rendered tooth crowns, we provide correlated cusp labels along the tooth row from the ultimate premolar to the molars to illustrate homologous cusp identification on different teeth. For instance, cusp B in P3 is considered as equivalent to the stylocone in the molars. The ultimate premolar can be considered as having a typical triconodont tooth pattern with the cusps aligned in a row on a transversely compressed tooth crown. M1 shows a transitional cusp arrangement, which is "obtuse-angled" and lies morphologically in between the premolars and the distal molars. Following the convention of tribosphenic and tribosphenic-like mammals, as well as their putative sister groups (Crompton and Jenkins 1968; Davis 2011, but see an alternative hypothesis in Rougier et al. 2003b), we consider cusp A to be equivalent to the paracone, cusp B to the stylocone, and cusp C to the metacone.

In occlusal view the outline of the upper molar has a skewed triangular shape. The embrasure between adjacent upper molars has a similar but reversed shape of a skewed triangle that matches the shape of the lower molar. The preparacrista is transversely straight, extending from cusp A to B. The postparacrista is longer and extends diagonally to cusp C or the metastyle (or C plus D) at the distobuccal corner in distal molars. This configuration is most characteristic of M2 and M3. Cusp B may be traced in all molars. Cusp C is discernable on M1–M3 of the holotype but fades away on M4–M6. Cusp C is not discernable on M2–M6 in the ZGY0053, which is partly attributable to the lower resolution of the CT-san of that specimen. From M1 to M3 of the holotype, cusp C migrates buccally away from cusp A. Cusp C may be interpreted as either lost or merged with cusp D on M4–M6 in *Lactodens sheni*. If this interpretation is correct, it implies that the metastyle may be homologized to cusp D or C plus D in *L. sheni*. On the preparacrista there is no cusp. The parastyle is small; it may also be lost or merged with cusp B in distal molars. The ectoflexus is shallow and the distal stylar cusp is low, extending mesiodistally along the buccal edge of the tooth crown; it is distinct on M2–M4 but nearly absent in distal molars. The cingulum is not strong but complete; in several teeth it was broken away. In buccal or lingual view, cusp A is not symmetrical; its mesial side is convex and steep, whereas its distal side is concave and more gently sloping. As revealed by CT-images for both the holotype and the new specimen, the upper molars have two roots, arranged mesiodistally. The roots are transversely wide (mesiodistally compressed), with the distal one being narrower than the mesial one; this is particularly distinct in M3–M5. A detailed description of the upper teeth of *Lactodens sheni* has been provided by Han and Meng (2016).

Lower teeth (Figs. 3, 5, 7): In the lower dentition, the incisors, canine, p2 and p4–m1 were preserved in the holotype of *Lactodens sheni* and described by Han and Meng (2016); the other teeth were not preserved or broken. In the ZGY0053 all the lower teeth (c, p1–p5, m1–m6) were
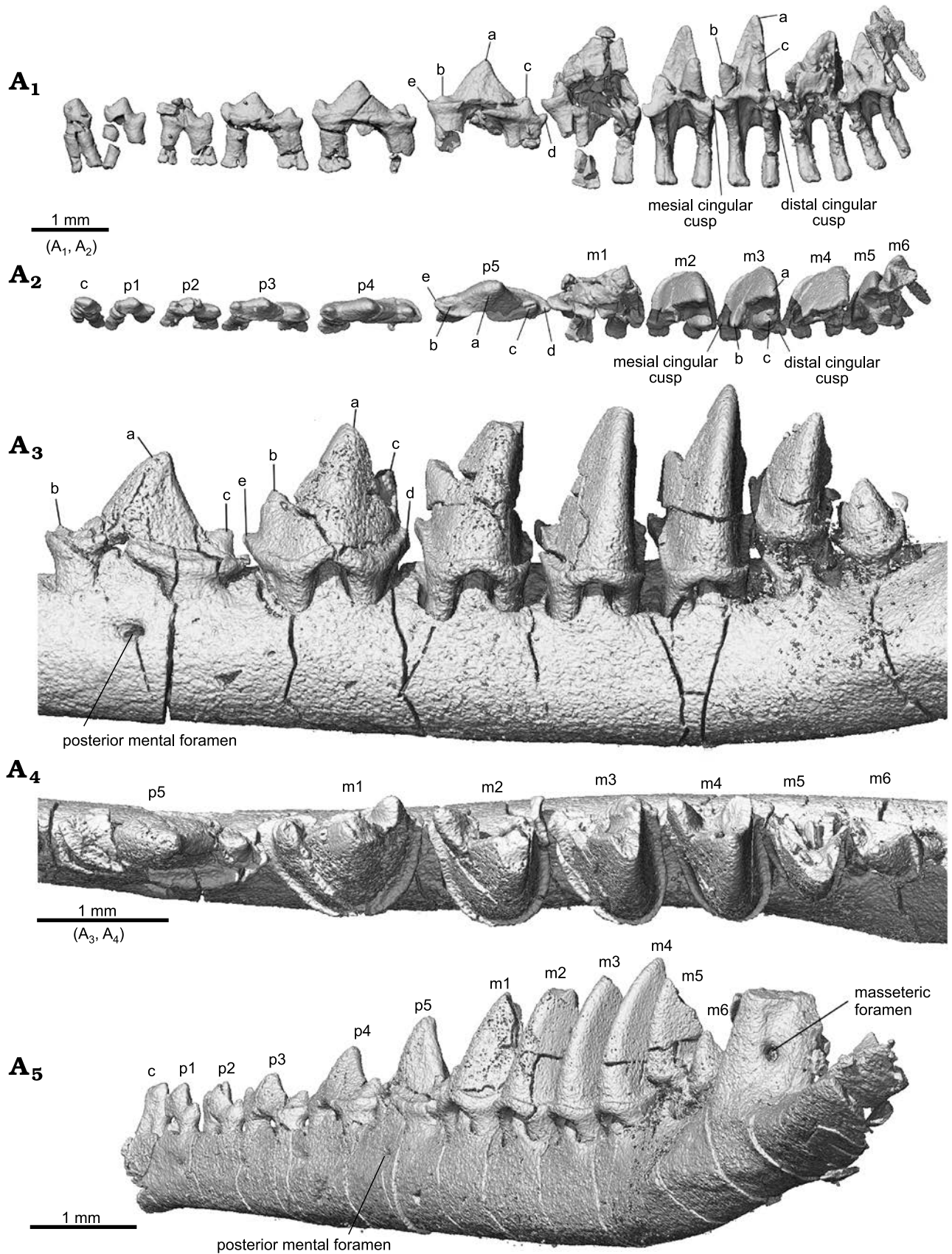
Fig. 5. Lower teeth of the trechnotherian mammal *Lactodens sheni* Han and Meng, 2016 (ZGY0053) from Aptian, Lower Cretaceous Jiufotang Formation of Dapingfang, Caoyang City, Liaoning Province, China), right c–m6 in lingual (A₁) and occlusal (A₂) views (with the dentary bone segmented away) and in posterobuccal view (A5), left p5–m6 in buccal (A₃) and occlusal (A₄) views. See also Figs. 3 and 7.

preserved in situ except for the right m6 that was displaced from its alveolus (Fig. 3A$_4$–A$_6$). ZGY0053 confirms that the lower canine is a small and double-rooted tooth with the roots closely packed. The first lower premolar (p1) has size and shape that lie intermediate between the canine and p2. The two roots of p1 are separated with the distal root being stronger than the mesial one (this is true for all lower premolars). The p1 has a simple tricuspid crown with three cusps aligned in a row as in a triconodont tooth. Cusp b is small and forms the mesial end of the crown. A ridge from cusp a descends distally to the mesial base of cusp c. In buccal or lingual view, the main part of cusp a is in the mesial half of the crown and cusp c is more distantly separated from cusp a than is cusp b. The p2 is similar to p1 but larger. The p3 is about twice the length of p1, confirming what has been known from the p3 impression left in the holotype. Except for being larger, it differs from p2 in having the distal portion (distal to cusp a) proportionally elongated; this is partly due to the development of a small distal cusp d. Weak cingulids also develop on the buccal and lingual sides of p3. The p4 is an enlarged version of p3 with the cingulids better developed and cusp a enlarged. The p5 and m1 are nearly identical to those in the holotype (Han and Meng 2016).

Identification of the premolars and molars in *Lactodens sheni* is based on tooth morphology. ZGY0053 confirms the morphological gradient from p5 to molars observed in the holotype. The m1 differs from p5 in having a much higher crown that is comparable to that of m2. Most distinctively, the three main cusps of m1 are arranged in a nearly 90° angle in occlusal view. The m1 is double-rooted, with the mesial root being mesiodistally longer than the distal one, which is opposite to the condition of p5. In addition, the roots of the premolars are widely separated and transversely compressed; the molar roots are mesiodistally compressed.

The lower molars gradually reduce tooth length and trigonid angle distally from m1 to m6. The m2–m4 are similar in general shape, with m4 being the tallest. The buccal cingulid on these teeth is complete; it forms a U-shape belt in occlusal view that starts from the mesial base of the paraconid (cusp b), extends around the crown, and ends at the distal base of the metaconid (cusp c). This U-shape cingulid reflects a buccally rounded crown base, which contrasts to the more angular outline of the crown that becomes more acute toward to the crown tip. The buccal portion of the cingulid is low; it ascends while extending lingually and ends as the mesial cingular cusp at the mesiolingual base and the distal cingular cusp (Cifelli and Gordon 1999; Cifelli and Madsen 1999) at the distolingual base of the crown. The two cingular cusps were also denoted as cusp e and d in the holotype (Han and Meng 2016; see references therein). The cingular cusps are much higher in position than the buccal portion of the cingulid; this reflects the fact that the buccal tooth crown is much higher than the lingual part. The lingual cingulid is weak or incomplete. The high tooth crown is pointed and leans distally. The lingual face of cusp a (protoconid) is flat or slightly concave, in contrasting to its labial convex

surface. In distal view (Fig. 5A$_3$), the buccal surface of cusp a curves dorsolingually from the cingulid toward the tip; this curved surface, along with a similar one but in opposite orientation from the upper molar, would suggest a curved path of occlusal movement during power stroke of orthal mastication. Cusps b and c are conical and high; they are closely positioned in comparison to those in m1. Cusp c is notably higher than cusp b. Cusp b leans mesially and cusp c is vertical or slightly leaning distally. In occlusal view, cusp b is mesiolingual to cusp a, while cusp c is lingual to the latter; thus, the mesial surface of the tooth crown extends mesioliangually with a curved (convex) slope, whereas the distal surface of the crown is transverse and nearly vertical. The distinctive cusp b and c are in sharp contrast to absence or weakly developed cusp B (B') and C in the upper molar. The paracristid between cusp a and b and the protocristid between cusp a and c are low, forming an open V-shape with the limb from cusp a (protoconid) being longer. Opposite to the outline of the upper molar, the distal surface of the lower molar is transversely straight, whereas the mesial one is diagonally stretched. The embrasure formed by adjacent lower molars takes the shape of the upper molar. The m5 is similar to m4 but smaller, and m6 is greatly reduced in size; the size changes are most distinctive in crown height and width.

In the holotype, because m2–m6 were broken, it remains unknown whether the interlocking pattern (defined as cusp d placed buccal to cusp e of the succeeding tooth; Kielan-Jaworowska et al. 2004) is present. The new specimen shows that the lower molars are not in close contact. Where the contact is present on the lingual sides of the tooth junction, cusp d is lingual to cusp e of the succeeding tooth. We consider that the interlocking pattern is not present in *Lactodens sheni*. The reconstruction of the lower molars of the holotype (Han and Meng 2016: fig. 9) is not accurate in that the distal teeth, particularly m6, were reconstructed a bit too large; the new specimen shows that m6 is much smaller than the one reconstructed in the holotype. In the holotype, there is no sign of successive tooth germs under any premolar and molar. The CT-scans of the holotype and new specimen confirm this observation (Fig. 2).

Although the lower teeth have been flipped 90° in the new specimen in preservation, their relative mesiodistal positions to the corresponding upper teeth remain nearly original, which helps to interpret the occlusal relationship of the upper and lower teeth. An interesting feature is that each upper molar is a half tooth mesial to the corresponding lower molar. For instance, in occlusion m1 bites in the embrasure between M1 and M2 so that the mesial half of m1 is in contact with the distal half of M1, whereas the distal half of m1 is in contact with the mesial half of M2 (Fig. 3). As a result of this occlusal relationship, the ultimate lower molar is a half tooth distal to the upper one. The same relationship is present in the zhangheotheriid *Origolestes lii* (Mao et al. 2020). This occlusal relationship differs from the tribosphenic dentition in which the upper molar is a half tooth distal to the lower one.

Remarks.—In the original report of *Lactodens sheni* (Han and Meng 2016) a thorough comparison was made between the holotype and other genera in Spalacotheriidae. In contrast, the comparison with zhangheotheriids was brief partly because the focus of that study was about *Lactodens* and its spalacotheriid relatives. In addition, the mandibular and dental morphologies of the Jehol zhangheotheriids were not fully revealed because of the preservation in which the upper and lower teeth are in occlusion and exposed only on the side so that the dental morphologies, particularly the occlusal view, in those Jehol Biota zhangheotheriids still remain equivocal.

With the reports of *Anebodon luoi* Bi, Zheng, Meng, Wang, Robinson, and Davis, 2016 (Bi et al. 2016) and *Origolestes lii* (Mao et al. 2020), particularly the latter, a solid base has emerged to permit a more detailed comparison between *Lactodens sheni* and zhangheotheriids. In the Jehol Biota, zhangheotheriids are more diverse, including *Zhangheotherium quinquecuspidens* Hu, Wang, Luo, and Li, 1997, and species of *Anebodon*, *Maotherium*, and *Origolestes*; they all came from the Yixian Formation, which is stratigraphically lower than the Jiufotang Formation where *Lactodens sheni* came from. The spalacotheriid *Akidolestes cifellii* Li and Luo, 2006, which is most similar to *Lactodens sheni* among Jehol "symmetrodontans", also originates from the Yixian Formation and considered as a "symmetrodontan" species (Li and Luo 2006). *Lactodens sheni* is so far the only spalacolestine from the Jiufotang Formation.

The following comparison is mainly between *Lactodens sheni* and *Origolestes lii*; additional elements of comparison can be found in Han and Meng (2016). For *L. sheni* the features we selected for comparison are based on the holotype and ZGY0053. The specimens represent two individuals that have similar size and age; the latter is inferred from fully erupted teeth that show little wear. The two specimens also show little difference in tooth and mandibular morphologies. For *O. lii* the features are based on the five specimens reported by Mao et al. (2020), with IVPP V13604 being the representative because it is better imaged.

The compared features have been, or could be, used as characters for systermatic and phylogenetic analyses of "symmetrodontans" (e.g., Li and Luo 2006; Sweetman 2008; Han and Meng 2016). Zhangheotheriids and spalacotheriids can be distinguished based on crown height and cusp angle (Cuenca-Bescós et al. 2014); we show that there are perhaps more mandibular and dental features that could characterize the two groups. These features were recovered together in a single individual so that they may be helpful in assisting identification of fragmentary material in which these features are not preserved together. With relatively more complete dental and mandibular features, we hope that *Lactodens sheni* may be used as a representative taxon for spalacolestines or spalacotheriids in future higher-level phylogenetic analyses involving "symmetrodontans". Similarly, *Origolestes lii* could be another useful representative for zhangheotheriids.

Mandible: *Masseteric fossa*: As the attachment site for the masseter, the masseteric fossa reflects the size and orientation of this muscle and bears on mastication abilities of the animal. Figures 3 and 6 show that the masseteric fossa of *Lactodens sheni* is quite different from that of *Origolestes lii*. In relation to the slender horizontal ramus of the mandible, the fossa expands abruptly posterior to the anterior ridge of the fossa and extends posteriorly to the mandibular condyle. In contrast, the masseteric fossa of *O. lli* gradually widens posteriorly and has a restricted size due to the inclined coronoid process and up-curved dentary peduncle for the condyle. In addition, the masseteric fossa is closed anteriorly by the masseteric ridge in *L. sheni*, but opens anteriorly in *O. lii*.

Pterygoid fossa: The pterygoid fossa on the medial side of the dentary in each taxon corresponds well to the masseteric fossa in size and shape. The fossa in *Lactodens sheni* Han and Meng, 2016, is larger and deeper than that of *Origolestes lii* and a ventral crest is distinct. The anterior edge of the fossa extends farther anteriorly, passing the mandibular foramen, whereas in *O. lii* the fossa ends anteriorly at the foramen. A similar difference has been noted between *Spalacolestes* and *Zhangheotherium* (Cifelli and Madsen 1999). As shown by the size of the fossae on both sides of the mandible, the jaw muscles (masseter and pterygoid) of *L. sheni* must be proportionally large. In addition to the size, the dorsal border of the pterygoid fossa in *O. lii* is bounded by an inclined dorsal ridge, which is parallel to the anterior ridge of the masseteric fossa; these two ridges indicate that the orientation of the jaw muscles is posteriorly reclined in *O. lii*. In contrast, the muscle orientation is more vertical in *L. sheni*.

Masseteric foramen: The masseteric foramen, also called the buccal (labial) mandibular foramen (Davis 2012), is present in both the holotype and the new specimen of *Lactodens sheni* but not in *Origolestes lii* and other zhangheotheriids. This foramen is absent in species of *Spalacolestes*, except for an extremely small nutrient foramen in one specimen (Cifelli and Madsen 1999). In phylogenetic analyses, absence of this foramen is considered as primitive (Mao et al. 2020, 2021; references therein). However, Davis (2012) pointed out that this foramen is present in some eutriconodontans (Cifelli et al. 1998), species of *Vincelestes* (Rougier 1993), *Arguimus* (Lopatin and Averianov 2006), *Kielantherium* (Dashzeveg and Kielan-Jaworowska 1984), the metatherians *Alphadon* and *Kokopellia* (Cifelli and Muizon 1997, 1998), the Recent marsupial species of *Petaurus*, the basal eutherian *Prokennalestes* (Kielan-Jaworowska and Dashzeveg 1989; Lopatin and Averianov 2017) and some Late Cretaceous eutherians (Archibald and Averianov 2006; Wible et al. 2009). Davis (2012) noted that these structures are usually small and probably represent nutrient foramina and considered the large masseteric foramen in peramurans to be autapomorphic and of uncertain function. However, Lopatin and Averianov (2017) showed that in species of *Prokennalestes* the masseteric foramen varied in size and

was large in some specimens. More evidence is needed to understand the function and phylogenetic significance of the masseteric foramen.

Coronoid process: In *Lactodens sheni* the coronoid process is broad and proportionally short. In contrast this process is a long bony strip in *Origolestes lii* (Mao et al. 2020: fig. S4H, I, S6), which extends posterior to the dorsal side, or even passes the level of the mandibular condyle. In addition, the tilting of the coronoid process (measured as the angle between the anterior border of the coronoid process and the horizontal alveolar line of all molars) is different in the two taxa. In *L. sheni* the anterior ridge of the process arises with a high angle so that an angular turn in relation to the horizontal ramus was formed. In *O. lii*, the anterior ridge of the process gradually ascends from the horizontal ramus in a gentle curve and the process inclines posteriorly. The coronoid features appear stable in zhangheotheriids where this region is preserved, such as *Zhangheotherium* (Hu et al. 1997), *Maotherium* (Rougier et al. 2003a; Ji et al. 2009), and *Kiyatherium* (Lopatin et al. 2010). In these genera the tilting angle of the process is about 40° (Han and Meng 2016).

Mandibular condyle: The mandibular condyle was described as having a short stem in *Lactodens sheni* based on direct observation of the holotype (Han and Meng 2016: fig. 10D). However, the CT-scan shows that there is thin bone ventral to the posterior base of the condyle; thus, a stem or neck may not correctly describe the morphology. The angular region of *Lactodens sheni* is squared with a thickened posteroventral corner (the angular end). The mandibular condyle is located at the posterodorsal corner of this square-shaped angular region and does not show a narrow neck separating it from the rest of the angular region. In describing the mandible of species of *Spalacolestes*, Cifelli and Madsen (1999) thought the condyle would have been situated at, or slightly below, the alveolar margin of the horizontal ramus, lower than in *Spalacotherium*. An alternative interpretation is that the mandible of species of *Spalacolestes* has a thickened angular end, similar to that of *L. sheni*, and its condyle is probably higher than the alveolar margin, as in *L. sheni*. The similar tooth morphology between *Spalacolestes* and *Lactodens* would imply similar mastication movements and justifies the alternative interpretation mentioned above. In contrast, the mandibular condyle of *Origolestes lii* is supported by a long and curved dentary peduncle that has a diameter that is similar to the condyle's diameter. The peduncle extends posterodorsally toward the tip of the coronoid process and forms a curved stem (curved condylar process; Averianov 2002). This morphology is present in species of *Zhangheotherium*, *Maotherium*, and *Kiyatherium*; a similar condition may also be present in *Spalacotherium* (Cassiliano and Clemens 1979).

Mandibular notch: The mandibular notch is the space between the coronoid process and the mandibular condyle. Because of the unique morphology of the condyle and coronoid process, this space is narrow in *Origolestes lii* and other zhangheotheriids. The opening of the mandibular notch is the narrowest region of the notch, also unique among mammals. This configuration is likely relevant to the biomechanical function of the jaw muscle/jaw joint complex. It appears that a short moment arm for the jaw muscles (relative to the condyle and glenoid joint as the axis) is present in zhangheotheriids. A quantitative analysis is beyond the scope of this study, but it could potentially reveal how these two types of mandibles, in association with the teeth, work biomechanically.

Mandibular foramen: The mandibular foramen is similar in *Lactodens sheni* and *Origolestes lii*, although in *O. lii* the foramen is located slightly higher partly because of the taller horizontal ramus and the presence of the Meckelian groove on the ventral side. A pocket is present posterior to the foramen, which increases the ventral portion of the pterygoid fossa in *Spalacolestes* (Cifelli and Madsen 1999) and *L. sheni* (Han and Meng 2016). This region, however, was easily broken as shown in other specimens (Fig. 3).

Mental foramen: Both taxa have multiple mental foramina but *Lactodens sheni* appears to have one or two more. Multiple mental foramina are present in other taxa, such as *Gobiotheriodon infinitus* (Trofimov, 1980) Averianov, 2002 (Averianov 2002). Rougier et al. (2003a) considered that *G. infinitus* resembles *Zhangheotherium quinquecuspidens* and that one of shared features is the slender mandible with multiple mental foramina (four or more). However, the number and size of the mental foramina are different in the two mandibles of the same individual of *L. sheni*. Of the mental foramina, it appears the posterior one has a constant size (the largest) and position (under p5) within the known mandibles of *L. sheni* (Figs. 3, 5, 6), it has been used as a character in phylogenetic analyses (Mao et al. 2020).

Meckelian groove: It has been widely accepted that a persistent Meckel's cartilage, as evidenced by the groove on the medial surface of the dentary, is present in several early mammalian groups (Meng et al. 2003). This has been confirmed by the ossified Meckel's cartilage (OMC) preserved in several taxa (Wang et al. 2001; Meng et al. 2003, 2011; Luo et al. 2007; Ji et al. 2009; Mao et al. 2020). In addition to the Jehol zhangheotheriids, a distinct Meckelian groove is present in other "symmetrodontans" (Cassiliano and Clemens 1979; Cifelli and Madsen 1999; Averianov 2002; Meng et al. 2003). *Lactodens sheni* does not have such a groove. There is a faint groove on the medial surface of the dentary of the ZGY0053 (Fig. 3) but such a faint groove is probably not present in the holotype (Fig. 6). This faint trace is by no means comparable to the distinct Meckelian groove in *Origolestes lii* (Fig. 6), which is another feature that distinguishes the two taxa as well as the families they represent.

Teeth: Dental formula: Although the tooth morphology of zhangheotheriids is considered more primitive than that of spalacotheriids, the tooth formula may provide a different signal. *Zhangheotherium* and *Spalacotherium* appear to be derived with respect to Spalacolestinae in the loss of one or more premolars (Cifelli 1999); this implies that the postcanine teeth reduction is an evolutionary trend in "sym-
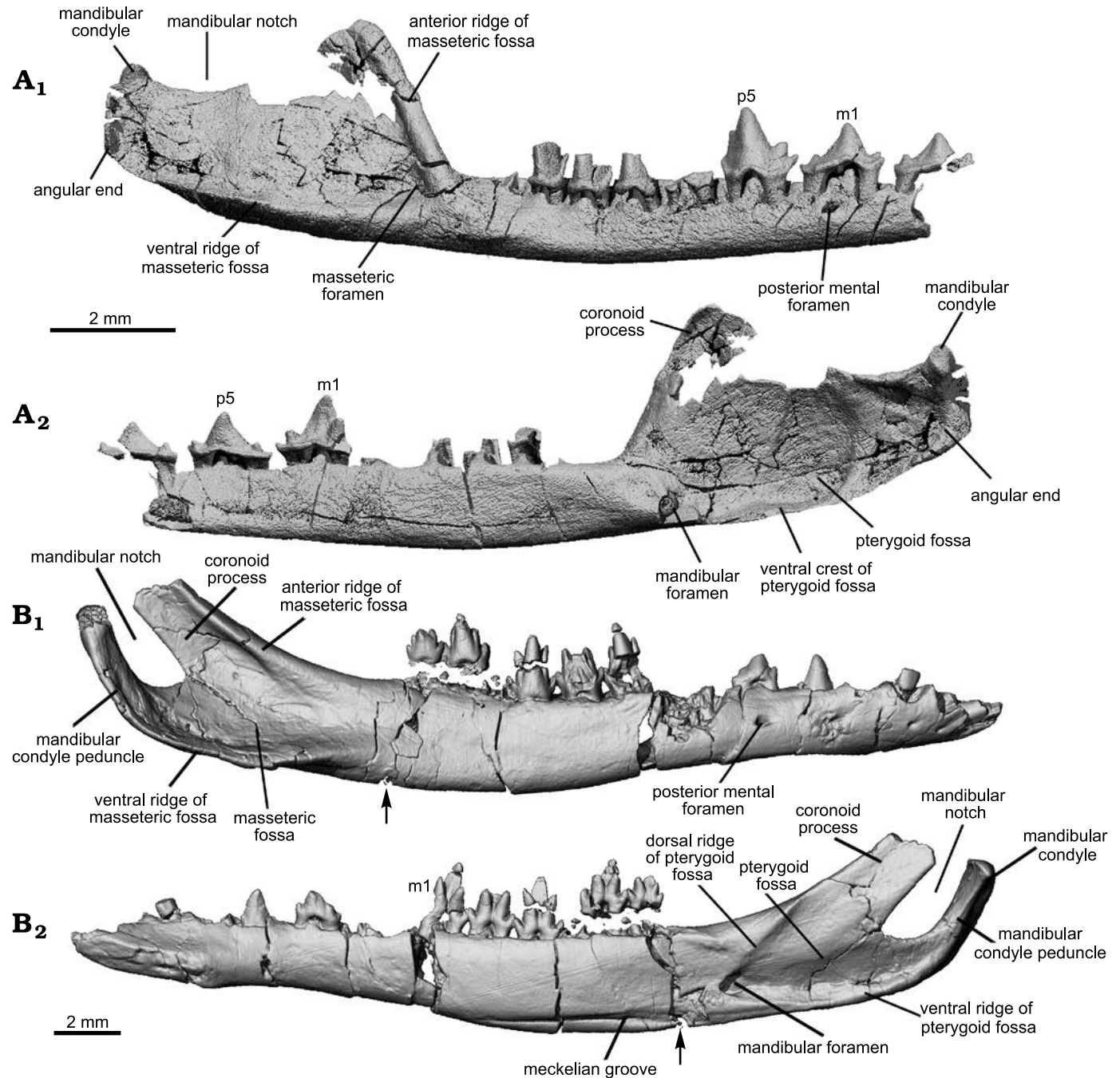
Fig 6. Comparison of the mandibular morphologies of *Origolestes* and *Lactodens*. **A.** *Lactodens sheni* Han and Meng, 2016 (holotype, HG-M016) from Aptian, Lower Cretaceous Jiufotang Formation of Shangheshou area, Caoyang City, Liaoning Province, China; posterior portion of the right mandible in buccal (A$_1$) and lingual (A$_2$) views. **B.** *Origolestes lii* Mao, Hu, Li, Wang, Chase, Smith, and Meng, 2020 (IVPP V13604) from Lower Cretaceous Lujiatun beds of the Yixian Formation of the Lujiatun locality, Beipiao County, Liaoning Province, China; right mandible in buccal (B$_1$) and lingual (B$_2$) views. The mandible in B was slightly displaced at the crack (marked with the arrow) and has been digitally restored (see Mao et al. 2020).

metrodontans". This reduction is present in *Maotherium sinense* Rougier, Ji, and Novacek, 2003 (I3-C1-P2-M4/i3-c1-p3-m6) (Rougier et al. 2003b) and *Maotherium asiaticum* Ji, Luo, Zhang, Yuan, and Xu Li, 2009 (I3-C1-P1-M5/i3-c1-p1-m6) (Ji et al. 2009); the latter represents an extreme condition in the premolar formula. This difference is best shown in the lower dentition partly because lower jaws are better documented in fossils. This difference is here shown again between *Lactodens sheni* (I3-C1-P3-M6/i3-c1-p5-m6) and *Origolestes lii* (I2-C1-P3-M4/i2-c1-p4-m5). Although the number of premolars is problematic for some species (Averianov 2002) or remains uncertain, such as in *Kuehneotherium* D.M. Kermack, K. Kermack, and Mussett, 1968 (Kermack et al. 1968; Gill 1974), the known record indicates that the tooth formula is diverse in "symmetrodontans".

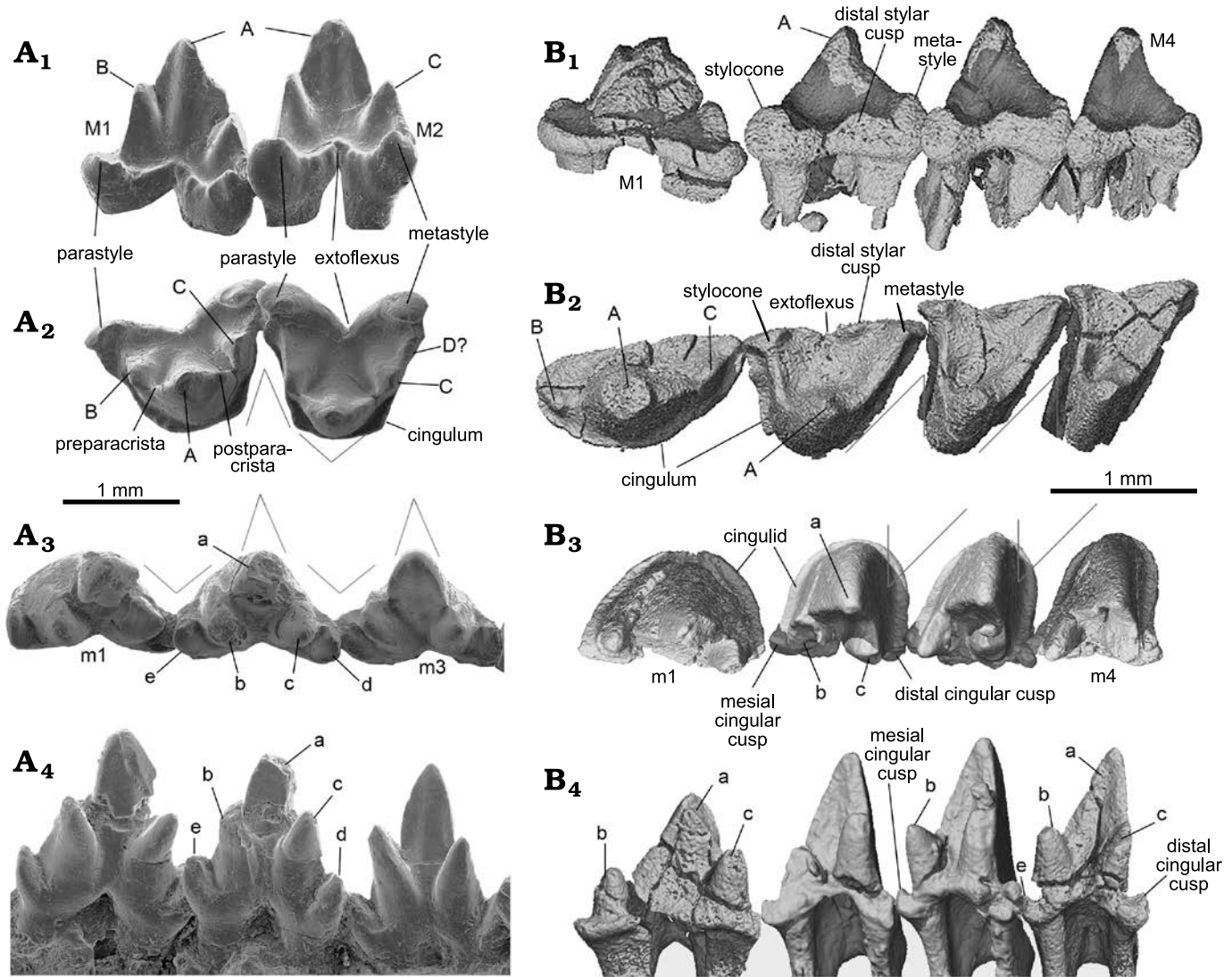*Molar outline*: The taxon name Symmetrodonta was proposed by Simpson (1925b: 560) based on the symmetrical

Fig. 7. Comparison of molars between of *Origolestes* and *Lactodens*. **A**. *Origolestes lii* Mao, Hu, Li, Wang, Chase, Smith, and Meng, 2020 (IVPP V13604) from Lower Cretaceous Lujiatun beds of the Yixian Formation of the Lujiatun locality, Beipiao County, Liaoning Province, China; upper molars (M1–M2) in buccal (A_1) and occlusal (A_2) views; lower molars (m1–m3) in occlusal (A_3) and lingual (A_4) views (modified from Mao et al. 2020). **B**. *Lactodens sheni* Han and Meng, 2016 (ZGY0053) from Aptian, Lower Cretaceous Jiufotang Formation of Dapingfang, Caoyang City, Liaoning Province, China; upper molars (M1–M4) in buccal (B_1) and occlusal (B_2) views; lower molars (m1–m4) in occlusal (B_3) and lingual (B_4) views. Image in B_1 has been vertically reversed for convenience of comparison. The lower teeth (m1–m4) in B_3 and B_4 were composite from better preserved left m2–m3 (reversed) and right dentitions (m1, m4). The angular lines indicate the symmetrical (*O. lii*) and asymmetrical (*L. sheni*) crown outline and the embrasure.

lower molar morphology "in allusion to the symmetrical triangular pattern which distinguishes the lower molars of this group from those of any other"; this was based primarily on *Spalacotherium*. This tooth symmetry was an issue of taxonomy; for instance, *Peralestes* was placed in Spalacotheriidae but its asymmetrical molar was inconsistent with other members, mainly *Spalacotherium* (Simpson 1928). When spalacolestines were later included in the group and especially when the three-dimensional views of the molar in various species became available, it was made clear that not all the teeth were symmetrical. In the occlusal, lingual, and buccal views of both upper and lower molars of *Origolestes lii*, the tooth is more or less symmetrical. In *Lactodens sheni*, the upper and lower molar outlines are clearly asymmetrical, with a shape of skewed triangle, espe-

cially in the occlusal view, as described above. As noted by Averianov (2002) the main trend of spalacotheriid evolution is toward an acute-angled molar pattern, with the mesial (prevallum) and distal (postvallum) shearing surfaces being in a more transverse position. This trend is particularly distinct for the mesial shearing crest of the upper molars and the distal one of the lower molars. The embrasure between two adjacent molars corresponds to the shape of the molar it receives.

Tooth morphology: In addition to dental formula and molar outline, which are better understood with both upper and lower dentitions, there are other dental differences between *Lactodens sheni* and *Origolestes lii*, as shown in Fig. 7. These dental characters have been discussed in detail when comparing zhangheotheriids and spalacotheriids

Table 2. Comparison of dental characters between *Lactodens sheni* Han and Meng, 2016, and *Origolestes lii* Mao, Hu, Li, Wang, Chase, Smith, and Meng, 2020.

	Characters	*Lactodens sheni*	*Origolestes lii*
Upper teeth	cusp A in buccal view	not symmetrical	symmetrical
	cusp C	indistinct or absent	distinct and conical
	cusp B	small and buccal	present and lingual
	parastyle	weak	strong and hooked
	metastyle	weak	strong and hooked
	extoflexus	shallow	deep
	preparacrista (prevallum)	long and continuous	short and notched
	postparacrista (postvallum)	long and continuous	short and notched
	distal stylar cusp	present	absent
Lower teeth	crown height (relative to length)	high	low
	buccal cingulid	complete	absent
	cusp e (mesial cingular cusp)	weak if present	distinct and conical
	cusp d (distal cingular cusp)	not conical	distinct and conical
	cusp b and c relative height	cusp b lower than c	cusp b higher than c
	number of canine roots	two	one

(Hu et al. 1997; Cifelli and Madsen 1999; Averianov 2002; Rougier et al. 2003a; Tsubamoto et al. 2004; Li and Luo 2006; Sweetman 2008; Cuenca-Bescós et al. 2014) so that we briefly list the differences in Table 2. Many of the compared dental and mandibular features have been used to diagnose Spalacotheriidae (Tsubamoto et al. 2004).

It should be noted that there are unsettled issues about cusp homologies, a subject that is beyond the scope of this study. For the purpose of comparison, we adopt the interpretation of Rougier et al. (2003b) that the cusp immediately mesial to cusp A is cusp B in zhangheotheriids, including *Origolestes lii* (Mao et al. 2020); this cusp has been considered as B' in *Zhangheotherium quinquecuspidens* (Hu et al. 2017). The issue concerning the nature of cusps B and B' in zhangheotheriids remains to be resolved.

Stratigraphic and geographic range.—Aptian, Lower Cretaceous Jiufotang Formation in Liaoning Province, China.

Conclusive remarks

Dentition.—Taking advantage of the full dentitions available from single individuals, we focus on a few features that are difficult to assess from isolated teeth or incomplete dentitions. The first point is the dental variation within a single tooth row. As we show above, the upper and lower molars at different loci vary in their size and shape. M1 has a wide angle in cusp arrangement and the angle decreases distally. In addition, the tooth crown morphologies differ notably in that M1 is less crested than other molars. If these teeth were preserved in isolation, they may be identified as from different taxa, as in the case of *Palaeoxonodon ooliticus* (Close et al. 2016). Under this scenario, if only M1 of *Lactodens sheni* was available, it might be identified as originating from a "symmetrodontan" with an obtuse-angled molar. This should raise caution on species previously identified based on isolated teeth. For instance, the holotype of *Mictodon*

simpsoni (UA16273; Fox 1984: 1204) was based on a left upper molar from the middle Upper Cretaceous Milk River Formation, Alberta, Canada, and this tooth was considered as "the first North American post-Jurassic 'obtuse-angled' symmetrodont to be discovered and is approximately 65 Ma younger than any earlier known North American 'obtuse-angled' species." In light of the dental variation of the tooth row in *L. sheni*, the identification of the holotype of *M. simpsoni* as M1 of a dentition with acute-angled distal molars cannot be ruled out. In general, the upper and lower dentitions are consistent with what Averianov and Lopatin (2008) have observed on dental variation in a tooth row of "symmetrodontans", which could result in different interpretations on isolated teeth, such as those of *Eurylambda aequicrurius* (Simpson 1925a; Rougier et al. 2003b), which has played an important role in understanding tooth evolution in mammals (Crompton and Jenkins 1968; Crompton 1971).

The second point is that in the tooth rows, M1/m1 show a transitional morphology from a triconodont-like premolar to a typical molar with reversed triangular cusp arrangement; this morphological gradient may provide a clue in understanding the cusp variations on molars. In general, the cusps of the premolars are relatively simple and can be readily compared to those of a triconodont tooth. M1/m1 retain the main cusps but these cusps are in an obtuse triangular arrangement (Figs. 3, 4, 7). As for most spalacotheriids (Cifelli and Madsen 1999), except for *Yaverlestes gassoni* (Sweetman 2008), the distal upper molars of *Lactodens sheni* have strong crests between the protoconid and lingual cusps but cusp C is weak or absent. If compared to M1 where cusp C is present between cusp A and a small distobuccal cusp (interpreted as the metastyle by its position), it is reasonable to assume that cusp C distally became weaker and located more buccally, until getting eventually lost in distal molars; whether it forms part of the metastyle at the distobuccal margin is uncertain. Similarly, the stylocone and cusp B can be compared between M1 and the distal molars.

Finally, in addition to the tooth-to-tooth occlusal relationship that has been examined in detail in interpreting tooth evolution toward the tribosphenic pattern (Crompton 1971; Davis 2011; Schultz and Martin 2014), the dentitions as a whole also provide information about tooth occlusion. In *Lactodens* (and *Origolestes* as well) the upper and lower dentitions from a single individual are available and preserved in nearly original occlusal relationship. Although the upper and lower molars are equal in number (6 to 6), the ultimate lower molar is a half tooth distal to its upper counterpart when the dentitions are in occlusion, or the ultimate upper molar fits in the embrasure between the ultimate and penultimate lower molars. This is in contrast to the dentition of the tribosphenic pattern, in which the ultimate upper molar is always a half tooth distal to the lower one because the protocone of the former must fit in the talonid basin of the ultimate lower molar; thus, the entire ultimate upper molar is distal to the trigonid of the ultimate lower molar. The same relationship is present in *Origolestes lii* and other "symmetrodontans" where the upper and lower dentitions are known from a single individual. In most cases there is at least one more lower molar compared to the upper molar count; in these forms the ultimate lower molar would be the distalmost tooth when the dentitions are in occlusion.

Regardless the complicated evolutionary pattern in the upper molar, the trigonid of the tribosphenic lower molar is presumably homologous to the entire lower molar of "symmetrodontans" and the main shearing facet (facet 1) in relation to the protoconid (cusp a) and metaconid (cusp c) remains continuously traceable throughout holotherians (Crompton and Jenkins 1968; Crompton 1971; Rougier et al. 2003b; Davis 2011; Schultz and Martin 2014). Thus, during the evolution from the reversed-triangular tooth to the tribosphenic pattern within trechnotherians, the ultimate lower molar would be the one that had to be lost in the dentition; or with the development of the talonid on the lower molar, the presence of the ultimate lower molar distal to the ultimate upper one became functionally meaningless. This perhaps indicates that the occlusal relationship of upper and lower teeth and the number of upper vs. lower teeth are coupled. A similar condition (at least one additional lower molar, compared to the upper molar count) may also be present in eutriconodontans, as shown in several taxa where the upper and lower dentitions from a single individual are unequivocally known (Ji et al. 1999; Hu et al. 2005b; Meng et al. 2011; Hou and Meng 2014). The ultimate lower molar as the distalmost tooth may be regarded as a primitive feature for trechnotherians.

Meckelian groove.—The evolution of the mammalian middle ear consists of at least two steps that involve complicated changes of the postdentary bones, jaw joint and basicranial region (Meng et al. 2011). The first step is from the mandibular middle ear to the transitional mammalian middle ear (TMME), which marks the separation of the postdentary bones from the dentary bone. The second step

is from the TMME to the definitive mammalian middle ear (DMME; Allin 1975; Allin and Hopson 1992), which is characterized by the resorption of the Meckel's cartilage and full separation of the auditory bones from the mastication process. Fossils of "symmetrodontans" document changes in the second evolutionary step in which the postdentary trough is absent, but the Meckelian groove is present in some taxa and held an OMC (Wang et al. 2001; Meng et al. 2003). The Meckelian groove on the medial surface of the dentary bone is observed in relatively early branching "symmetrodontans" (Simpson 1925a; Cassiliano and Clemens 1979; Hu et al. 1997; Cifelli and Madsen 1999; Averianov 2002; Meng et al. 2003; Ji et al. 2009). Recently, Mao et al. (2020) reported several specimens of *Origolestes lii* that have well-preserved lower jaws and OMCs. These specimens convincingly demonstrate that the groove accommodated a sizable OMC that was probably held in the groove by soft tissue in life. However, as a close relative of *O. lii* in the Jehol Biota, *Lactodens sheni* does not have the Meckelian groove. Absence of the groove has also been recognized in other spalacotheriids where the dentary bone is adequately preserved, such as species of *Spalacolestes* (Cifelli and Madsen 1999), *Heishanlestes* (Hu et al. 2005a), and *Yaverlestes* (Sweetman 2008). The non-grooved condition, as represented by *L. sheni*, suggests lack of the OMC in adults, which further implies acquisition of the DMME in spalacotheriids.

A Meckelian groove similar to that of *Origolestes lii* is present in many stem-group therian mammals that are dentally more advanced than "symmetrodontans", such as species of *Palaeoxonodon* (Close et al. 2016; Panciroli et al. 2018), *Amphitherium* (Prothero 1981; Butler and Clemens 2001), *Nanolestes* (Martin 2002), peramurans (Davis 2012), *Kielantherium* (Dashzeveg and Kielan-Jaworowska 1984), and *Prokennalestes* (Kielan-Jaworowska and Dashzeveg 1989). It may be inferred that an OMC similar to that of *Origolestes* was present in these forms and that the DMME of therians could have been derived from the configuration documented in *O. lii*. Thus, the possible acquisition of the DMME in spalacotheriids implies at least another independent evolution of the fully suspended middle ear that took place within "symmetrodontans", provided that spalacotheriids form a monophyletic group. Independent evolution of the DMME refers to the processes in which the postdentary bones became separated from the dentary, and which involve two steps, as mentioned above. In *O. lii*, the bony contact between the OMC and auditory bones was lost but the OMC is still present, perhaps functioning as a support structure for the auditory bones through a connection of soft tissue (Mao et al. 2020). This could be viewed as either the end state of the TMME or the beginning of the DMME, which is different from the condition present in eutriconodontans, such as *Liaoconodon hui*; in the latter, a substantial contact existed between the OMC on the one hand and the long anterior processes of the malleus and ectotympanic on the other hand (Meng et al. 2011). Thus,

the evolutionary change from the *O. lii* condition to that of *Lactodens sheni* can be narrowed down to the loss of the OMC in adult and securely housing of the auditory bones at the basicranial region. A similar process could have taken place independently in therians.

Morphological disparity.—As already noted, spalacotheriids differ from zhangheotheriids in having higher crowned molars with a more acute angle in cusp arrangement in the middle of the tooth series (Cuenca-Bescós et al. 2014). As also noted by Cifelli and Madsen (1999), species of *Zhangheotherium* (*Maotherium* as well) is strikingly atypical in having features such as the complete lack of cingula on the lower molars. Primitively, *Zhangheotherium quinquecuspidens* has rounded, conical molar cusps that lack connecting crests (Hu et al. 1997). These features show that zhangheotheriids have not achieved the dental specialization characteristic for Spalacotheriidae (Averianov 2002). Our comparison shows that the two families are similar mainly in the development of main cusps (cusp a, b, and c) on the lower molars, but they differ in nearly all other aspects of dental morphology. Furthermore, the dental structures are consistently associated with the mandibular structures. The size, shape and orientation of the coronoid process, the mandibular condyle, and the masseteric and pterygoid fossae are distinctive between the two families. It appears that the mandibular configuration in each species has been specialized in its own way. In particular, the mandibular structures of *Origolestes lii* are quite unusual in that the mandibular condyle has a long and curved peduncle and that the coronoid process is a narrow strip that extends posteriorly over the condyle and defines a narrow mandibular notch. These features appear unique among mammals. *Lactodens sheni* is the only spalacolestine from a stratigraphically younger unit and the several species of zhangheotheriids are from the Yixian Formation in the Jehol Biota, but the morphological differences between them may not be explained by the temporal difference. If spalacotheriids were derived from zhangheotheriids, as suggested by some phylogenetic analyses (Han and Meng 2016), the evolutionary changes of the teeth and mandibles would be remarkable. The observed differences probably indicate a deep split between the two groups, perhaps deeper than previously thought, and such a deep split has been shown by the phylogenetic analysis of Averianov et al. (2013).

The general tooth morphology and small body size of *Lactodens sheni* and *Origolestes lii* suggest an insectivorous lifestyle. Han and Meng (2016) speculated on the dietary adaptation of *L. sheni* based on its dental and mandibular morphologies and body size. Compared to *O. lii*, whose conical teeth appear specialized for piercing or puncturing, the dentition with well-developed crests in *L. sheni* suggests embrasure shearing. These two kinds of dental morphologies, along with the mandibular features and orientations of the jaw muscles (inferred from the bony structures), form two complexes that show different biomechanical dynam-

ics of mastication in food processing, which would argue for different habitat preferences between these two species and between spalacotheriids and zhangheotheriids. A more sophisticated analysis about the biomechanics of the teeth and mandibles, as done for species of *Morganucodon* and *Kuehneotherium* (Gill et al. 2014), may better reveal dietary preferences between the two forms. It has also been suggested that the long-term survival of spalacotheriids is linked to their ability to consume food resources not readily available to other mammals in the ecosystem (Averianov 2002). Although this is difficult to test, the coexistence of *L. sheni* and zhangheotheriids with other mammals (multituberculates, eutriconodontans, therians; Meng 2014) in the Jehol Biota, as well as their high masticatory disparities, are consistent with partitioning of the food resources.

Acknowledgements

References

Allin, E.F. 1975. Evolution of the mammalian middle ear. *Journal of Morphology* 147: 403–437.

Allin, E.F. and Hopson, J.A. 1992. Evolution of the auditory system in Synapsida ("mammal-like reptiles" and primitive mammals) as seen in the fossil record. *In*: D.B. Webster, A.N. Popper, and R.R. Fay (eds.), *The Evolutionary Biology of Hearing*, 587–614. Springer, New York.

Archibald, J.D. and Averianov, A.O. 2006. Late Cretaceous asioryctitherian eutherian mammals from Uzbekistan and phylogenetic analysis of Asioryctitheria. *Acta Palaeontologica Polonica* 51: 351–376.

Averianov, A.O. 2002. Early Cretaceous symmetrodont mammal *Gobiotheriodon* from Mongolia and the classification of Symmetrodonta. *Acta Palaeontologica Polonica* 47: 705–716.

Averianov, A.O. and Lopatin, A. 2008. "Protocone" in a pretribosphenic mammal and upper dentition of tinodontid "symmetrodontans. *Journal of Vertebrate Paleontology* 28: 548–552.

Averianov, A.O. and Lopatin, A.V. 2011. Phylogeny of triconodonts and symmetrodonts and the origin of extant mammals. *Doklady Biological Sciences* 436 (1): 32–35.

Averianov, A.O., Martin, T., and Lopatin, A.V. 2013. A new phylogeny for basal Trechnotheria and Cladotheria and affinities of South

American endemic Late Cretaceous mammals. *Naturwissenschaften* 100: 311–326.

Bi, S.-D., Zheng, X.-T., Meng, J., Wang, X.-L., Robinson, N., and Davis, B. 2016. A new symmetrodont mammal (Trechnotheria: Zhangheotheriidae) from the Early Cretaceous of China and trechnotherian character evolution. *Scientific Reports* 6: 1–9.

Butler, P.M. and Clemens, W.A. 2001. Dental morphology of the Jurassic holotherian mammal Amphitherium, with a discussion of the evolution of mammalian post-canine dental formulae. *Palaeontology* 44: 1–20.

Cassiliano, M. and Clemens, W. 1979. Symmetrodonta. *In*: J. Lillegraven, Z. Kielan-Jaworowska, and W. Clemens (eds.), *Mesozoic Mammals: The First Two-thirds of Mammalian History*, 150–161. University of California Press, Berkeley.

Chang, S.C., Zhang, H., Renne, P.R., and Fang, Y. 2009. High-precision 40Ar/39Ar age for the Jehol Biota. *Palaeogeography, Palaeoclimatology, Palaeoecology* 280: 94–104.

Cifelli, R.L. 1990. Cretaceous mammals of southern Utah. III. Therian mammals from the Turonian (early Late Cretaceous). *Journal of Vertebrate Paleontology* 10: 332–345.

Cifelli, R.L. 1999. Therian teeth of unusual design from the mid-Cretaceous (Albian–Cenomanian) Cedar Mountain Formation of Utah. *Journal of Mammalian Evolution* 6: 247–270.

Cifelli, R.L. and de Muizon, C. 1997. Dentition and jaw of *Kokopellia juddi*, a primitive marsupial or near-marsupial from the medial Cretaceous of Utah. *Journal of Mammalian Evolution* 4: 241–258.

Cifelli, R.L. and de Muizon, C. 1998. Marsupial mammal from the Upper Cretaceous North Horn Formation, central Utah. *Journal of Paleontology* 72: 532–537.

Cifelli, R. and Gordon, C. 1999. Symmetrodonts from the Late Cretaceous of Southern Utah, and comments on the distribution of archaic mammalian lineages persisting into the Cretaceous of North America. *Geology Studies, Brigham Young University* 44: 1–16.

Cifelli, R.L. and Madsen, S.K. 1986. An Upper Cretaceous symmetrodont (Mammalia) from southern Utah. *Journal of Vertebrate Paleontology* 6: 258–263.

Cifelli, R.L. and Madsen, S.K. 1999. Spalacotheriid symmetrodonts (Mammalia) from the medial Cretaceous (upper Albian or lower Cenomanian) Mussentuchit local fauna, Cedar Mountain Formation, Utah, USA. *Geodiversitas* 21: 167–214.

Cifelli, R.L., Davis, B.M., and Sames, B. 2014. Earliest Cretaceous mammals from the western United States. *Acta Palaeontologica Polonica* 59: 31–53.

Cifelli, R.L., Rowe, T.B., Luckett, W.P., Banta, J., Reyes, R., and Howes, R.I. 1996. Fossil evidence for the origin of the marsupial pattern of tooth replacement. *Nature* 379: 715–718.

Close, R.A., Davis, B.M., Walsh, S., Wolniewicz, A.S., Friedman, M., and Benson, R.B. 2016. A lower jaw of *Palaeoxonodon* from the Middle Jurassic of the Isle of Skye, Scotland, sheds new light on the diversity of British stem therians. *Palaeontology* 59 155–169.

Crompton, A. 1971. The origin of the tribosphenic molar. *In*: D. Kermack and K. Kermack (eds.), Early Mammals. *Zoological Journal of the Linnean Society* 50: 65–87.

Crompton, A. and Jenkins, F.A. 1968. Molar occlusion in Late Triassic mammals. *Biological Reviews* 43: 427–458.

Crompton, A. and Sita-Lumsden, A. 1970. Functional significance of the therian molar pattern. *Nature* 227: 197–199.

Cuenca-Bescós, G., Canudo, J.I., Gasca, J.M., Moreno-Azanza, M., and Cifelli, R.L. 2014. Spalacotheriid "symmetrodonts" from the Early Cretaceous of Spain. *Journal of Vertebrate Paleontology* 34: 1427–1436.

Dashzeveg, D. and Kielan-Jaworowska, Z. 1984. The lower jaw of an aegialodontid mammal from the Early Cretaceous of Mongolia. *Zoological Journal of the Linnean Society* 82: 217–227.

Davis, B.M. 2011. Evolution of the tribosphenic molar pattern in early mammals, with comments on the "dual-origin" hypothesis. *Journal of Mammalian Evolution* 18: 227–244.

Davis, B.M. 2012. Micro-computed tomography reveals a diversity of Per-

amuran mammals from the Purbeck Group (Berriasian) of England. *Palaeontology* 55: 789–817.

Ensom, P. and Sigogneau-Russell, D. 2000. New symmetrodonts (Mammalia, Theria) from the Purbeck Limestone Group, Lower Cretaceous, southern England. *Cretaceous Research* 21: 767–779.

Fox, R.C. 1976. Additions to the mammalian local fauna from the upper Milk River Formation (Upper Cretaceous), Alberta. *Canadian Journal of Earth Sciences* 13: 1105–1118.

Fox, R.C. 1984. A primitive, "obtuse-angled" symmetrodont (Mammalia) from the Upper Cretaceous of Alberta, Canada. *Canadian Journal of Earth Sciences* 21: 1204–1207.

Fox, R.C. 1985. Upper molar structure in the Late Cretaceous symmetrodont Symmetrodontoides Fox, and a classification of the Symmetrodonta (Mammalia). *Journal of Paleontology* 59: 21–26.

Gill, P.G. 2004. A new symmetrodont from the Early Cretaceous of England. *Journal of Vertebrate Paleontology* 24: 748–752.

Gill, P.G. 1974. Resorption of premolars in the early mammal *Kuehneotherium praecursoris*. *Archives of Oral Biology* 19: 327–328.

Gill, P.G., Purnell, M.A., Crumpton, N., Brown, K.R., Gostling, N.J., Stampanoni, M., and Rayfield, E.J. 2014. Dietary specializations and diversity in feeding ecology of the earliest stem mammals. *Nature* 512: 303–305.

Han, G. and Meng, J. 2016. A new spalacolestine mammal from the Early Cretaceous Jehol Biota and implications for the morphology, phylogeny, and palaeobiology of Laurasian "symmetrodontans". *Zoological Journal of the Linnean Society* 178: 343–380.

He, H.Y., Wang, X.L., Zhou, Z.H., Wang, F., Boven, A., Shi, G.H., and Zhu, R.X. 2004. Timing of the Jiufotang Formation (Jehol Group) in Liaoning, northeastern China, and its implications. *Geophysical Research Letters* 31: L12605.

Hopson, J.A. 1994. Synapsid evolution and the radiation of non-eutherian mammals. *In*: R.S. Spencer (ed.), *Major Features of Vertebrate Evolution*, 190–219. The Paleontological Society, Knoxville.

Hopson, J.A. and Crompton, A. 1969. Origin of mammals. *In*: T. Dobzhansky, M.K. Hecht, and W.C. Steere (eds.), *Evolutionary Biology*, 16–72. Appleton-Century-Crofts, New York.

Hou, S. and Meng, J. 2014. A new eutriconodont mammal from the Early Cretaceous Jehol Biota of Liaoning, China. *Chinese Science Bulletin* 59: 546–553.

Hu, Y.-M., Fox, R.C., Wang, Y.-Q., and Li, C.-K. 2005a. A new spalacotheriid symmetrodont from the Early Cretaceous of northeastern China. *American Museum Novitates* 3475: 1–20.

Hu, Y.-M., Meng, J., Wang, Y.-Q., and Li, C.-K. 2005b. Large Mesozoic mammals fed on young dinosaurs. *Nature* 433: 149–152.

Hu, Y.-M., Wang, Y.-Q., Li, C.-K., and Luo, Z.-X. 1998. Morphology of dentition and forelimb of *Zhangheotherium*. *Vertebrata PalAsiatica* 36 (2): 102–125.

Hu, Y.-M., Wang, Y.-Q., Luo, Z.-X., and Li, C.-K. 1997. A new symmetrodont mammal from China and its implications for mammalian evolution. *Nature* 390: 137–142.

Jäger, K., Luo, Z.-X., and Martin, T. 2020. Postcranial skeleton of *Henkelotherium guimarotae* (Cladotheria, Mammalia) and locomotor adaptation. *Journal of Mammalian Evolution* 27: 349–372.

Ji, Q., Luo, Z.-X., and Ji, S.-A. 1999. A Chinese triconodont mammal and mosaic evolution of the mammalian skeleton. *Nature* 398: 326–330.

Ji, Q., Luo, Z.-X., Zhang, X., Yuan, C.-X., and Xu, L. 2009. Evolutionary development of the middle ear in Mesozoic therian mammals. *Science* 326: 278–281.

Kermack, D.M., Kermack, K., and Mussett, F. 1968. The Welsh pantothere *Kuehneotherium praecursoris*. *Zoological Journal of the Linnean Society* 47: 407–423.

Kielan-Jaworowska, Z. and Dashzeveg, D. 1989. Eutherian mammals from the Early Cretaceous of Mongolia. *Zoologica Scripta* 18: 347–355.

Kielan-Jaworowska, Z., Cifelli, R.L., and Luo, Z.-X. 2004. *Mammals From the Age of Dinosaurs: Origins, Evolution, and Structure*. 630 pp. Columbia University Press, New York.

Li, G. and Luo, Z.-X. 2006. A Cretaceous symmetrodont therian with some monotreme-like postcranial features. *Nature* 439: 195–200.

Lopatin, A.V. and Averianov, A.O. 2006. Revision of a pretribosphenic mammal Arguimus from the Early Cretaceous of Mongolia. *Acta Palaeontologica Polonica* 51: 339–349.

Lopatin, A.V. and Averianov, A.O. 2017. The stem placental mammal *Prokennalestes* from the Early Cretaceous of Mongolia. *Paleontological Journal* 51: 1293–1374.

Lopatin, A.V., Averianov, A.O., Maschenko, E., and Leshchinskiy, S. 2010. Early Cretaceous mammals of Western Siberia: Zhangheotheriidae. *Paleontological Journal* 44: 573–583.

Lopatin, A.V., Maschenko, E., Averianov, A.O., Rezvyi, A.S., Skutschas, P., and Leshchinskiy, S. 2005. Early Cretaceous mammals from Western Siberia: Tinodontidae. *Paleontological Journal* 39: 523–524.

Luo, Z.-X., Chen, P., Li, G., and Chen, M. 2007. A new eutriconodont mammal and evolutionary development in early mammals. *Nature* 446: 288–293.

Mao, F., Hu, Y., Li, C., Wang, Y., Chase, M.H., Smith, A., and Meng, J. 2020. Integrated hearing and chewing modules decoupled as shown in a new Cretaceous mammal. *Science* 367: 305–308.

Mao, F., Zhang, C., Liu, C., and Meng, J. 2021. Fossoriality and evolutionary development in two Cretaceous mammaliamorphs. *Nature* 592: 577–582.

Martin, T. 2002. New stem-lineage representatives of Zatheria (Mammalia) from the Late Jurassic of Portugal. *Journal of Vertebrate Paleontology* 22: 332–348.

Matsuoka, H., Kusuhashi, N., and Corfe, I.J. 2016. A new Early Cretaceous tritylodontid (Synapsida, Cynodontia, Mammaliamorpha) from the Kuwajima Formation (Tetori Group) of central Japan. *Journal of Vertebrate Paleontology* 36 (4): e1112289.

Meng, J. 2014. Mesozoic mammals of China: implications for phylogeny and early evolution of mammals. *National Science Review* 1: 521–542.

Meng, J., Hu, Y., Wang, Y., and Li, C. 2003. The ossified Meckel's cartilage and internal groove in Mesozoic mammaliaforms: implications to origin of the definitive mammalian middle ear. *Zoological Journal of the Linnean Society* 138: 431–448.

Meng, J., Wang, Y.-Q., and Li, C.-K. 2011. Transitional mammalian middle ear from a new Cretaceous Jehol eutriconodont. *Nature* 472: 181–185.

Nessov, L. 1997. *Cretaceous Non Marine Vertebrates of Northern Eurasia.* 218 pp. Institute of Earth Crust, University of Sankt Petersburg, Saint Petersburg.

Pan, Y., Sha, J., Zhou, Z., and Fürsich, F.T. 2013. The Jehol Biota: definition and distribution of exceptionally preserved relicts of a continental Early Cretaceous ecosystem. *Cretaceous Research* 44: 30–38.

Panciroli, E., Benson, R.B., and Butler, R.J. 2018. New partial dentaries of amphitheriid mammal *Palaeoxonodon ooliticus* from Scotland, and posterior dentary morphology in early cladotherians. *Acta Palaeontologica Polonica* 63: 197–207.

Patterson, B. 1955. A symmetrodont mammal from the Early Cretaceous of northern Texas. *Fieldiana: Zoology* 37: 689–693.

Patterson, B. 1956. Early Cretaceous mammals and the evolution of mammalian molar teeth. *Fieldiana-Geology* 13: 1–105.

Prothero, D.R. 1981. New Jurassic mammals from Como Bluff, Wyoming, and the interrelationships of non-tribosphenic Theria. *Bulletin of the American Museum of Natural History* 167: 277–326.

Rougier, G.W. 1993. Vincelestes neuquenianus *Bonaparte (Mammalia, Theria), un primitivo mamífero del Cretácico inferior de la Cuenca Neuquina*. 720 pp. Ph.D. Dissertation Thesis, Universidad Nacional de Buenos Aires, Buenos Aires.

Rougier, G.W., Ji, Q., and Novacek, M.J. 2003a. A new symmetrodont mammal with fur impressions from the Mesozoic of China. *Acta Geologica Sinica-English Edition* 77: 7–14.

Rougier, G.W., Spurlin, B.K., and Kik, P.K. 2003b. A new specimen of *Eurylambda aequicrurius* and considerations on "symmetrodont" dentition and relationships. *American Museum Novitates* 3398: 1–16.

Ruf, I., Maier, W., Rodrigues, P.G., and Schultz, C.L. 2014. Nasal anatomy of the non-mammaliaform cynodont *Brasilitherium riograndensis* (Eucynodontia, Therapsida) reveals new insight into mammalian evolution. *The Anatomical Record* 297: 2018–2030.

Schultz, J.A. and Martin, T. 2014. Function of pretribosphenic and tribosphenic mammalian molars inferred from 3D animation. *Naturwissenschaften* 101: 771–781.

Sigogneau-Russell, D. 1983. A new therian mammal from the Rhaetic locality of Saint-Nicolas-de-Port (France). *Zoological Journal of the Linnean Society* 78: 175–186.

Sigogneau-Russell, D. and Ensom, P. 1998. *Thereuodon* (Theria, Symmetrodonta) from the Lower Cretaceous of North Africa and Europe, and a brief review of symmetrodonts. *Cretaceous Research* 19: 445–470.

Simpson, G.G. 1925a. Mesozoic Mammalia, II: *Tinodon* and its allies. *American Journal of Science* 10: 451–470.

Simpson, G.G. 1925b. Mesozoic Mammalia, III: Preliminary comparison of Jurassic mammals except multituberculates. *American Journal of Science* 10: 451–470.

Simpson, G.G. 1928. *A Catalogue of the Mesozoic Mammalia in the Geological Department of the British Museum*. 215 pp. Trustees of the British Museum, London.

Sweetman, S.C. 2008. A spalacolestine spalacotheriid (Mammalia, Trechnotheria) from the Early Cretaceous (Barremian) of southern England and its bearing on spalacotheriid evolution. *Palaeontology* 51: 1367–1385.

Tsubamoto, T., Rougier, G.W., Isaji, S., Manabe, M., and Forasiepi, A.M. 2004. New Early Cretaceous spalacotheriid symmetrodont mammal from Japan. *Acta Palaeontologica Polonica* 49: 329–346.

Wang, Y., Hu, Y., Meng, J., and Li, C. 2001. An ossified Meckel's cartilage in two Cretaceous mammals and origin of the mammalian middle ear. *Science* 294: 357–361.

Wang, H., Meng, J., and Wang, Y. 2019. Cretaceous fossil reveals a new pattern in mammalian middle ear evolution. *Nature* 576: 102–105.

Wible, J.R., Rougier, G.W., Novacek, M.J., and Asher, R.J. 2009. The eutherian mammal *Maelestes gobiensis* from the Late Cretaceous of Mongolia and the phylogeny of Cretaceous Eutheria. *Bulletin of the American Museum of Natural History* 327: 1–123.

Yang, S., He, H., Jin, F., Zhang, F., Wu,Y., Yu, Z., Li, Q., Wang, M., O'Connor, J. K., and Deng, C. 2020. The appearance and duration of the Jehol Biota: Constraint from SIMS U-Pb zircon dating for the Huajiying Formation in northern China. *Proceedings of the National Academy of Sciences* 117: 14299–14305.